DEPARTMENT OF THE ARMY CORPS OF ENGINEERS

BEACH EROSION BOARD
OFFICE OF THE CHIEF OF ENGINEERS

STABILITY OF OSCILLATORY LAMINAR FLOW ALONG A WALL

TECHNICAL MEMORANDUM NO. 47

STABILITY OF OSCILLATORY LAMINAR FLOW ALONG A WALL

TECHNICAL MEMORANDUM NO. 47

BEACH EROSION BOARD

CORPS OF ENGINEERS

JULY 1954

FOREWORD

The depth to which sand movement caused by wave action extends is of importance in many beach studies involving littoral transport. This problem has lately received more attention as recent evidence tends to indicate that appreciable sediment movement may take place in depths as great as 60-70 feet. One of the first steps in placing an outer limit to the depths at which sand movement by wave action may be expected to occur, is the formulation of a criterion for the condition at which flow at or near the bed is unstable (i.e. turbulent). The study discussed in the following report represents the initial portion of work done on this problem; it consists of a theoretical and laboratory analysis of the stability of oscillatory flow along a wall.

This report has been prepared at the University of California at Berkeley in pursuance of contract DA-49-055-eng-17 with the Beach Erosion Board which provides in part for the study of the mechanism of sand transport by wave motion. The author of this report, Huon Li, is a Research Engineer at that institution, and this report is derived from thesis work performed toward the completion of his doctoral degree at that university.

Views and conclusions stated in this report are not necessarily those of the Beach Erosion Board.

This report is published under authority of Public Law 166, 79th Congress, approved July 31, 1945.

TABLE OF CONTENTS

		Page
Chapter I.	Introduction	1
	1. Laminar Flow and Turbulent Flow	
	2. Existing Theories on the Cause of Transition from Laminar to Turbulent	
	3. Transition due to Finite Disturbance	
	4. Stability of Laminar Flow due to Small Incidental Disturbances and Its Transition to Turbulence	
	5. Theory of Transition	
	6. Critical Reynolds Number	
	7. Phenomenon of Transition	
	8. Effects of Roughness on Transition	
	9. Scope of the Present Investigation	
Chapter II.	Oscillatory Boundary Layer	6
	10. Surface Wave Motion and Its Boundary Layer Flow	
	11. Orbital Motion	
	12. Oscillatory Motion Near a Smooth Bottom	
	13. Oscillatory Motion Near a Rough Bottom	
Chapter III.	Experimental Equipment and Procedure	12
	14. General Considerations	
	15. Experimental Set-up	
	16. Procedure and Range of Experiment	
	17. Observation of Transition from Laminar to Turbulent Motion by the Trails of Dye	
Chapter IV.	Experimental Results	16
	18. Smooth Bottom	
	19. Rough Bottom, Two-Dimensional	
	20. Rough Bottom, Three-Dimensional	
Chapter V.	Discussion of the Experimental Results	27
	21. Limitation of the Experiments	
	22. On the Length Scales	
	23. On the Smooth Bottom	
	24. On the Rough Bottom	
	25. Classification of the Smooth and Rough Boundaries	
	26. Notes on the Experiment	
Chapter VI.	Conclusions	32
	References	33
	Appendix	35

LIST OF SYMBOLS

a' = length of semi-major axis of orbit of water particle (ft.)

a'_b = length of semi-major axis of orbit of water particle near or at bottom (ft.)

b' = length of semi-minor axis of orbit of water particle (ft.)

D = diameter of pipe (ft.)

d = depth of water (ft.)

d_1 = total displacement of oscillatory plate (stroke) (ft.)

H = wave height (ft.)

L = wave length (ft.)

T = wave period (sec.)

t = time (sec.)

U = velocity component of flow in x-direction (ft./sec.)

u_z = horizontal velocity of orbit of water particle (ft./sec.)

V = velocity component of flow in z-direction (ft./sec.)

v_z = vertical velocity of orbit of water particle (ft./sec.)

U_o = maximum velocity of the oscillatory bottom (ft./sec.)

W = velocity component of flow in y-direction (ft./sec.)

x = coordinate in horizontal direction

y = coordinate in horizontal direction

z = coordinate in vertical direction; depth below the mean position of the surface orbit

R = Reynolds number, $R = \dfrac{\omega^{1/2} d_1}{\nu^{1/2}}$

R_ϵ = Reynolds number, $R_\epsilon = \dfrac{\omega d_1 \epsilon}{\nu}$

β = characteristic scale of the oscillatory motion

$$\beta = \left(\frac{\omega}{2\nu}\right)^{1/2}\left(\frac{1}{ft.}\right)$$

LIST OF SYMBOLS (cont'd)

δ_1 = boundary layer thickness (ft.)

ϵ = roughness diameter (ft.)

μ = dynamic viscosity (lb. sec./ft.^{2})

ν = kinematic viscosity (ft.^{2}/sec.)

ρ = density (lb. sec.^{2}/ft.^{4})

ω = angular velocity (1/sec.)

ξ = horizontal displacement of orbit water (ft.)

η = vertical displacement of orbit motion (ft.)

STABILITY OF OSCILLATORY LAMINAR FLOW ALONG A WALL

by
Huon Li
University of California, Berkeley, California

CHAPTER I

INTRODUCTION

1. Laminar Flow and Turbulent Flow

In 1883 Osborne Reynolds(1)* first demonstrated qualitatively the characteristics of a turbulent flow by the following experiment which is still being used today. He introduced dye into the water which was flowing in a glass tube with a smooth entry. At a small rate of flow the filament of the dye extended down the tube in a straight line. As the rate of flow increased up to a certain stage, the straight line motion began to break down. The straight line motion is termed laminar, and the motion after breakdown is called turbulent. These two different types of flow appear also in boundary layer flow, jet flow, and many other cases.

Laminar and turbulent flow are essentially different in character. For instance, the pressure gradient is proportional to the first power of the velocity for a laminar pipe flow, but approximately to the second power of the velocity for turbulent flow. The velocity distribution in a pipe section is parabolic if the flow is laminar, but approximately logarithmic if the flow becomes turbulent. The skin-friction of ships and airplanes also are different when the flow along their surface is turbulent and when it is laminar.

In laminar flow the fluid particles acting as units are of molecular size, and the particles are constrained to motion in parallel paths by viscosity. In turbulent flow much larger masses of fluid move together as units, breaking down in time and mixing with other masses of fluid. The motion becomes very complicated, and it is impossible to predict the detail of the instantaneous flow pattern. However, important relationships of turbulent flow may be obtained by a statistical analysis of turbulent flow records. It is the randomness of the motion that distinguishes the turbulence from secondary flows and periodical wave motions.

2. Existing Theories on the Cause of Transition from Laminar to Turbulent.

How and under what circumstances does turbulence occur? This question has attracted great attention in the past seventy years. The problem was first posed by Rayleigh and Stokes in 1887(2). Since then it has been one of the major problems in hydrodynamics. Although valuable contributions have been made by Prandtl(3), Tollmien(4), Schlichting(5), Lin(6) and many others, the question still remains one of considerable dispute. There are two schools of thought regarding the cause of the transition from laminar to turbulent motion. One school assumes that the transition is the result of a definite instability of the laminar flow in which infinitely small incidental disturbances have the tendency to grow in time. The other

* Numbers refer to reference listed on page 33.

regards as unstable also a motion which is stable for infinitely small incidental disturbances, but is liable to become and stay unstable if subjected to disturbances of finite magnitude.

3. Transition Due to Finite Disturbance

The theory of finite disturbance dates back to Reynolds(7) and was developed by Schiller(8), Taylor(9), and others. Mathematical investigations of such finite disturbances are based on considerations of energy or vorticity which depend on the second power of the disturbance. Four characteristic causes for the transition have been pointed out by Taylor(9): (1) Conditions at the leading edge, (2) roughness of the surface, (3) turbulence in the stream when there is a reverse pressure gradient, and (4) condition arising in the boundary layer after separation. These effects are in general combined so that it is difficult to tell which one is the sole cause of a given transition.

4. Stability of Laminar Flow Due to Small Incidental Disturbances and Its Transition to Turbulence

Many investigators have attempted to solve the theoretical problem of the stability of laminar flow by determining what conditions are necessary to cause infinitely small disturbances to increase with time. This work dates back to Lord Rayleigh(10). The most successful case was Taylor's treatment of the flow between two rotating cylinders(11). His work was verified by experiments(11)(12). This is known as a typical case of the instability of a fluid motion where centrifugal force plays a dominant part. A specific problem of the stability of laminar boundary layer flow near a flat plate without pressure gradient was studied by Tollmien(4). The problem was idealized by assuming a layer of constant thickness, and the distribution of mean velocity was computed by Blasius. It was shown that a small disturbance of a certain wave length would be amplified in a critical layer, whereas the disturbances of a shorter or longer wave length would be damped provided the Reynolds number of the boundary layer was greater than a certain limiting value. The calculation was repeated and extended by Schlichting(13)(14). Lin(6) undertook a revision of the mathematical theory of the stability of two-dimensional parallel flow and a clarification of some features of the Tollmien theory. This theory, also, was extended to compressible flow by Lees(15), Dunn and Lin(16), and to free boundary flow by Lessen(17). In recent years the Tollmien theory has been verified experimentally by Schubauer and Stramstad(18) for a boundary layer flow on a flat plate and by Liepmann(19) for flows on a flat plate and a curved surface. It seems that the validity and applicability of the Tollmien theory are now beyond question.

The theory of stability of laminar motion for small disturbances give only the criterion indicating whether the laminar flow is stable or not. The transition is not directly given, for the linearized differential equation cannot show the breakdown of the laminar flow.

5. Theory of Transition

It appears to the writer that the aforementioned two schools of thought are not contradictory to each other. In fact, each method of attack deals with a different phase of the basic cause which changes the flow from laminar into turbulent flow. The mechanics of transition itself has not been described mathematically, but it is believed that the transition depends essentially on the nonlinear character of the equation of motion. It seems that two different types of mechanisms exist: (1) Sufficiently large disturbance (either original or amplified from the small incidental disturbances) which break down into individual eddies, and (2) a discontinuity becomes unstable and rolls up into individual eddies. The first case is similar to the breakdown of a surface wave. The second case can be demonstrated by the unstable character of a vortex-sheet of ideal flow. For a plane vortex-sheet, a small sinusoidal disturbance can be found which makes it roll up in the manner as shown below. The vorticity becomes more and more concentrated in the rolled-up portion, and then breaks down to small eddies.

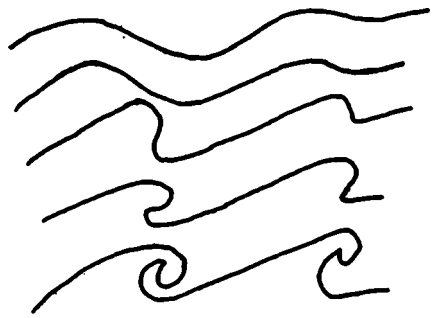

The ideal case should be modified by the effect of viscosity for the real fluid. On the other hand, the formation of the eddies does not necessarily represent the beginning of turbulence. Flow becomes turbulent only when the eddies move away from the location of origin, and this occurs at a certain Reynolds number.

6. Critical Reynolds Number

In pipe flow, Reynolds number, $\frac{U_m D}{\nu}$, (U_m is mean velocity, D is diameter of the pipe, and ν is the kinematic viscosity of the fluid) has been found to be a criterion between laminar and turbulent flow. When this Reynolds number reaches a certain value, the laminar flow breaks down into turbulence. Unfortunately, this upper limit of laminar flow is indefinite, as it depends on the following conditions:

1. Initial quietness of the flow and condition of pipe entrances

2. Roughness of the pipe

The lower critical Reynolds number defines a condition below which all disturbances entering the flow from any source eventually will be damped out by viscosity. This Reynolds number sets a limit below which the laminar

flow will always occur and has a value of about 2100.

The above results in pipe flow can be related to the study of stability and transition. The lower critical Reynolds number of the pipe flow corresponds to the minimum critical Reynolds number of the laminar motion for the stability investigation. This critical Reynolds number should be constant for a certain basic flow, The upper critical Reynolds number of the pipe flow can be regarded as the critical Reynolds number of transition. This critical Reynolds number is expected to vary, depending on the finite disturbance as well as the amplification of the small disturbances.

7. Phenomenon of Transition

It is believed that the transition is a combined picture of laminar and turbulent motion. This phenomenon was observed by the writer in an open channel flow of oil*. At laminar state no irregular disturbance was observed at the oil surface. However, if the rate of flow increased to a certain value , the flow became irregular at a certain point and at a certain instant of time. Those disturbances look like a "body of turbulent flow" bursting upon the flow. The more the flow rate increased, the shorter were the time intervals and the larger was the disturbed area. This development went on until the entire flow became turbulent.

But putting a condenser type of pressure pick-up at the bottom of the flume, the "body of turbulent flow" was detected. Oscillographic records were obtained to prove the existence of this transition.

Emmons(20), observing the boundary layer transition on a water-table analogy to supersonic flow, points out that the transition is not a clearly defined phenomenon. Instead, it is rather an intermittent process. The laminar layer is disturbed by the outside disturbances. When the disturbances reach a certain degree, a turbulent "burst" occurs. This turbulent "spot" moves along with the fluid and gradually fans out, making turbulent all before it. The farther downstream, the larger is the number of turbulent spots which have been developed upstream, and consequently, the larger percent of time the particular point is turbulent. Emmons develops a probability theory for predicting what percentage of time each position of the plate will be turbulent. This observation is quite similar to the above observation made in the oil channel, except that the "body of turbulent flow" is much larger than Emmons' turbulent "spot" and the movement of the "body of turbulent flow" in the oil is different from that observed by Emmons.

*This study is a part of turbulence research program under the supervision of Professors H. A. Einstein and L. M. Grossman, at the University of California, Berkeley.

8. Effects of Roughness on Transition

The effects of a single roughness on the transition have been investigated recently by Dryden(21), Hama and Tani(22). It is believed that the effects of combined roughness are more complicated. It appears to the writer that the roughness effects the transition in the following ways:

1. It changes the boundary condition and, thus, changes the velocity distribution of the basic flow.

2. For a very small roughness, the irregularities of the boundary create some small disturbances which may be amplified according to the stability theory for small disturbances.

3. If separation of the flow occurs at an individual roughness, the unstable wakes may contribute to the transition.

4. When the flow passes the roughness element, the centrifugal force may affect the stability of the motion.

9. Scope of the Present Investigation

The purpose of this thesis is to study the transition from laminar to turbulent flow in an oscillatory boundary layer near the solid bottom caused by a surface wave. However, the observations were made at a plate oscillating in still water for the sake of experimental convenience. The relationships between these two flow conditions are discussed, and the experimental results including the observation on both smooth and rough surfaces are given.

CHAPTER II

OSCILLATORY BOUNDARY LAYER

10. Surface Wave Motion and Its Boundary Layer Flow

Studies on beach and shore line processes indicate that most of the sediment movement along a coast by current and wave action takes place in and near the surf zone. Recent evidence, however, indicates that appreciable movement appears to be taking place in depths as great as 60 feet, and possibly greater. The extent of such movement by wave action at these greater depths depends on whether the oscillatory velocity of the water near the bed is sufficiently large to dislodge and transport the material. This velocity is a function of the height and period of the wave and of the water depth. One of the first steps in placing an outer limit to the depths at which sand movement along the ocean bed by wave action might be expected to occur is the formulation of a criterion for the condition at which flow at or near the bed becomes unstable (turbulent). It is well known that the irrotational theory can be applied fairly well to the entire surface wave motion except to a very thin layer adjacent to the solid boundaries. Near the solid boundaries the viscous effect can not be neglected compared with the inertia forces, no matter how small the viscosity of the fluid. But this layer near the boundary can be treated according to the boundary layer theory.

The thin boundary layer plays a very important role in studying the flow problem. Flow energy is dissipated in this layer, and especially the skin friction is the direct effect of the presence of this layer. The wave motion near the solid bottom has been found to approximate very closely a simple harmonic motion. The stability of the laminar boundary layer and its transition for this type of motion is important in many respects, one of which is the determination of sediment transport along the bottom for which the existence of turbulence is a governing factor. A review of the literature indicates that little has been done in this field. It is, therefore, the purpose of the present investigation to determine experimentally the factors and relationships governing the transition of an oscillatory laminar boundary layer over smooth and rough beds.

11. Orbital Motion

The motion of the individual particles for the wave motion of small amplitude is known as orbital motion(23). The horizontal and vertical displacement from its mean position at a distance z (measured negatively downward) below the still water surface are:

$$\xi = \frac{1}{2} H \frac{\cosh 2\pi(d + z)/L}{\sinh 2\pi d/L} \cos 2\pi\left(\frac{x}{L} - \frac{t}{T}\right) \qquad (1)$$

$$\eta = \frac{1}{2} H \frac{\sinh 2\pi(d + z)/L}{\sinh 2\pi d/L} \sin 2\pi\left(\frac{x}{L} - \frac{t}{T}\right)$$

where

H = wave height

d = depth of water, measured from the still-water level to the bottom

z = depth below the mean position of the surface orbit

x = horizontal coordinate

L = wave length

T = wave period

t = time

From Equation (1), the semi-orbital amplitudes of the water particle motion are:

$$a' = \frac{1}{2} H \frac{\cosh 2\pi (d \pm z)/L}{\sinh 2\pi d/L}$$
$$b' = \frac{1}{2} H \frac{\cosh 2\pi (d \pm z)/L}{\sinh 2\pi d/L} \qquad (2)$$

The horizontal and vertical velocity of the water particle can be obtained by differentiating Equation (1) with respect to time; one has

$$u_z = \frac{\partial \xi}{\partial t} = \frac{H \cosh 2\pi (d \pm z)/L}{T \sinh 2\pi d/L} \sin 2\pi \left(\frac{x}{L} - \frac{t}{T}\right) \qquad (3)$$
$$v_z = \frac{\partial \eta}{\partial t} = \frac{- H \sinh 2\pi (d \pm z)/L}{T \sinh 2\pi d/L} \cos 2\pi \left(\frac{x}{L} - \frac{t}{T}\right)$$

According to Equation (3), if the bottom friction is neglected the horizontal and vertical components of a water particle velocity at the bottom are:

$$u_z = \frac{\pi H}{T \sinh 2\pi d/L} \sin 2\pi \left(\frac{x}{L} - \frac{t}{T}\right) \qquad (4)$$
$$v_z = 0$$

If we let $\omega \frac{2\pi}{T}$, the angular velocity, and $a'_b = \frac{1}{2} H \frac{1}{\sinh 2\pi d/L}$ the semi-orbit amplitudes of the water particle motion at the bottom, Equation (4) becomes

$$u_z = -\omega a'_b \sin (\omega t - 2\pi x/L) \qquad (5)$$
$$v_z = 0$$

This is a simple harmonic motion relative to the bottom. The above derivations can only be applied to ideal flow. Near the bottom the viscosity effect cannot be neglected.

In the real case, the velocity of a water particle should be zero at the solid bottom. It is believed that the potential theory applies to the entire flow except a very thin layer adjacent to the solid boundaries. At a very short distance from the bottom, the velocity of the water particle is

$$u_z \doteq \omega a'_b \sin(\omega t - 2\pi x/L)$$
$$v_z \doteq 0 \tag{6}$$

Where a'_b is defined as before. The study of the characteristics of the wave motion near the solid boundaries is in itself a very interesting problem. However, in practice it is rather difficult to set up an experimental model for the oscillatory wave motion near a solid bottom, since the model must have a scale of the same order of magnitude as that of the prototype.

12. Oscillatory Motion Near a Smooth Bottom

Over a smooth flat bottom, the equations for the oscillatory motion are, with neglect of the non-linear inertia terms, pressure gradient and viscous effect in the x-direction.

$$\frac{\partial U}{\partial t} = \nu \frac{\partial^2 U}{\partial z^2} \tag{7}$$
$$v = W = 0$$

Let us suppose that the fluid lies on the positive side of the xy-plane, and the motion is due to an oscillation.

$$U = \omega a'_b \sin(\omega t - 2\pi x/L) \tag{8}$$

of a rigid and smooth surface at the xy-plane. If the fluid extends to infinity towards the z-direction, i.e. when

$$z \longrightarrow \infty, \quad U = 0 \tag{9}$$

we have a solution

$$U = U_o e^{-\beta z} \sin(\omega t - \beta z - 2\pi x/L) \tag{10}$$

with

$$U_o = \omega a'_b \tag{11}$$

$$\beta = \left(\frac{\omega}{2\nu}\right)^{1/2} \tag{12}$$

Since Equation (10) indicates that the velocity decreases very rapidly away from the boundary one can consider practically that only a thin layer adjacent to the boundary is in motion. For instance, for $\beta z = 4.6$, the amplitude of the oscillatory velocity reduces to about one percent. Therefore, a length scale

$$\delta_1 = 4.6 \frac{1}{\beta} = 6.5\sqrt{\frac{\nu}{\omega}} \tag{13}$$

can be defined as a boundary layer thickness.

The motion caused by the oscillation according to Equation (8) is similar to the wave motion near a solid boundary. In the above analysis the motion is created by an oscillatory bottom and is transmitted to the fluid by viscosity. For water as fluid for the range of periods tested, the layer affected by this motion is very thin due to the inertia of the fluid. In the previous case, discussed in Section 11 the fluid moves according to Equation (6) over the still bottom. Viscosity will prevent the occurrence of fluid motion immediately at the bottom, but the thickness of the fluid layer affected by friction is small and of the same order as given by Equation (13).

Experimentally, it is impractical to study the motion caused by the oscillation according to Equation (8) in the desired range of conditions. Therefore, the motion that is due to an oscillation of the type

$$U = U_o \sin \omega t \tag{14}$$

of a rigid and smooth surface at the xy-plane is studied experimentally. For this case the solution is:

$$U = U_o e^{-\beta z} \sin(\omega t - \beta z) \tag{15}$$

The motion which is described by Equation (15) is different from that of Equation (10). The latter is a function of x while the former is independent of x . In view of Equation (14) the experimental study of this investigation is only applicable to a very large wave length of surface wave motion.

If the boundary layer thickness δ_1 is to be chosen as the length scale, U_o as the characteristic velocity, we can define a Reynolds number as

$$R\delta_1 = \frac{U_o \delta_1}{\nu} \tag{16}$$

or

$$R\delta_1 = \text{const.}\,\omega^{1/2} d_1/\nu^{1/2} \tag{17}$$

with

$$d_1 = 2\,a'_b \tag{18}$$

Where d_1 is the total displacement of the oscillatory motion of the solid surface. In analogy to the steady parallel flow, one would expect that the oscillatory laminar boundary layer may break down at a critical Reynolds number under certain conditions. It is proposed that this critical Reynolds number is given by

$$R = \omega^{1/2} d_1 / \nu^{1/2} \tag{19}$$

The experimental results given in Section 18 agree well with this prediction.

13. Oscillatory Motion Near a Rough Bottom

It is impossible to find the mathematical solution of a laminar flow near a rough plate. The difficulty lies in the following points:

1. The nonlinear inertia terms for flow over a rough plate cannot be neglected.

2. The rough surface is usually of a very complicated geometry.

3. If any separation occurs, the real boundary conditions are changed.

Although the theoretical solution cannot be found, it may be possible to compare two systems of flow by using the similitude arguments. The dynamic similarity between geometrically and kinematically similar systems require that all homologous forces in the two systems should have the same ratio. In the present case, only inertia and the viscous force get into the flow picture. Therefore, the Reynolds number is the only criterion of dynamic similarity for the two systems of flow.

The question arises now how to define the Reynolds number for the oscillatory motion near a rough bottom. It is believed that $U_0 = \frac{1}{2}\omega d_1$ may still be used as characteristic velocity, while the roughness scale may be used as characteristic length in analogy to the steady flow problem. Thus the critical Reynolds number may be expected to have the form

$$R_\epsilon = \frac{\omega d_1 \epsilon}{\nu} \tag{20}$$

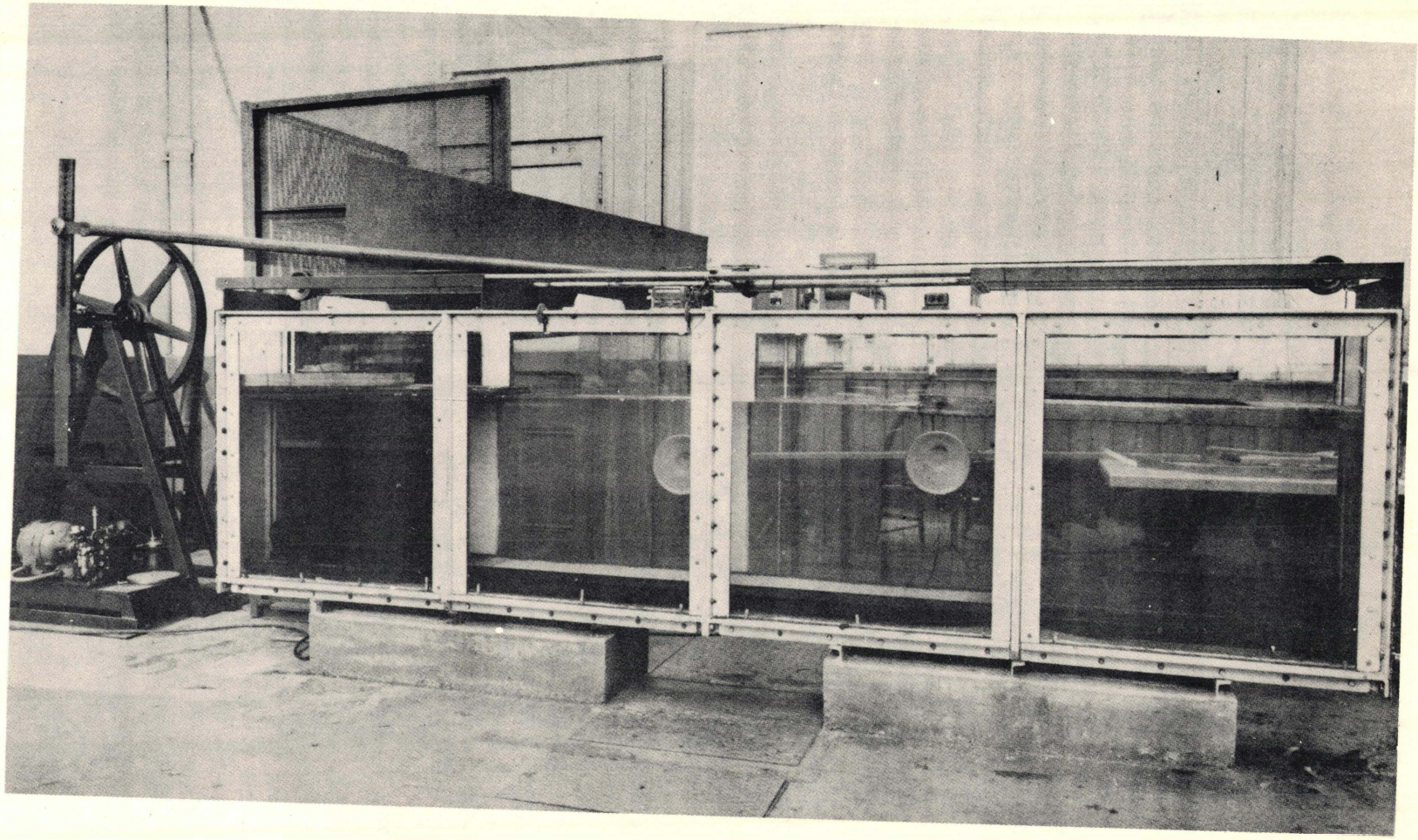

ARRANGEMENT OF THE EXPERIMENTAL SET-UP
FIGURE 1

CHAPTER III

EXPERIMENTAL EQUIPMENT AND PROCEDURE

14. General Considerations

As mentioned previously, evidence indicates that sediment movement along the ocean bottom occurs at depth of about 60 feet, and possibly at even greater depths. The relative motion between the water and bed with wave motion under prototype conditions (waves of 0.4 to 60 seconds period and 0.5 to 10 feet in height in water 60 feet in depth, or even larger) were computed and used as the basis of this experimental study. Obviously, the relative motion between water and bed for these prototype conditions could not be realized in a laboratory wave channel. These conditions could be obtained, however, by oscillating a plate in still water with the range and amplitude and period as computed by wave theory. A channel with an oscillating bottom, therefore, was designed based on the following considerations:

1. The motion of the bottom must be close to simple harmonic.

2. Any movable mechanical parts must create as little vibration of flow disturbance as possible.

3. A wide range of the frequency and the amplitude of the oscillatory motion must be available.

15. Experimental Setup

Figure 1 shows the general arrangement of the experimental equipment. The channel was 12 feet long, 3 feet deep, and 1 foot wide, made of steel plate and angles with four large panels of glass. At the bottom of the flume, a 6 feet by 11-1/2-inche movable steel plate resting on six pairs of rollers was installed. Two thin steel bands were fastened at both ends of the movable plate, and through four pulleys located at the upper and lower corners of each end of the flume the two bands joined together to a movable head on top of the flume. This well-guided head was driven by a crank mechanism and performed close to a simple harmonic motion. An A. C. motor provided the driving power of the mechanism. The angular velocity was controlled by a variable speed reducer and also by changing the size of the driving pulley. The total displacement of the movement was controlled in a range from 2-1/2 inches to 4 feet by adjusting the eccentric arm. The range of speeds covers from 1.0 to 150 cpm.

This arrangement had the following advantages:

1. The speed (angular velocity) and the amplitude of the oscillatory motion were easy to control over a large range.

2. The movable parts submerged in the water were reduced to a minimum.

3. The movement was well guided at any position.

4. The mechanical vibration was reduced to a minimum due to separation of the motor from the flume.

On the other hand, this setup did not give exactly a true simple harmonic motion. The maximum deviation of the displacement from the ideal harmonic motion was about 2 percent for the largest stroke. The difference was small at smaller stroke values.

Procedure and Range of Experiment

The experiments were carried out in three different groups:

1. Smooth bottom

2. Rough bottom: half round wooden strips and steel rods (two-dimensional case)

3. Rough bottom: sand and gravel (three-dimensional case)

For each experiment the type of bed roughness and the total displacement d_1 (stroke) were chosen. Then the bottom was oscillated at a low frequency and the flow pattern viewed by dropping potassium permanganate crystals from the water surface to the moving bottom. The crystals left a trail of dye in the water which was constantly deformed during the motion, and the undissolved remainder of the dye was deposited on the moving bottom where it gradually dissolved completely into a flat dense cloud with longitudinal streaks, the total height of which was up to about one-quarter inch for the smooth case (this height varied according to the frequency of the motion). The frequency of the oscillation next was gradually increased until these streaks suddenly curled up and disappeared, indicating the development of turbulence. The details of observation will be presented in the next article.

At that critical limit the speeds and the total displacement were recorded. The experiment was repeated for various total displacements, water depths, and bed roughness conditions. In each experiment the temperature of the water also was recorded. The experimental conditions covered the following ranges:

Bottom Condition	Roughness Element	Roughness Size	Water Depth (ft.)	Frequency (cpm)	Total Displacement (ft.)
Smooth	Wax applied to the surface		0.233-1.884	4.56-108	0.667-4.0
Two-Dimensional	Half round, Wooden strip	1-1/4" 3/4" 3/8"	0.445-1.892	1.66-99	
	Round steel rod	3/64"			

Bottom Condition	Roughness Element	Roughness Size	Water Depth (ft.)	Frequency (cpm)	Total Displacement (ft.)
Three-Dimensional	Sand	0.00308'			
		0.00090'			
	Gravel	0.0453'	0.289-1.966	1.62-64	0.208-4.0
	Polystyrene pellets	0.0104'			

17. Observation of Transition from Laminar to Turbulent Motion by the Trails of Dye

The following is a detailed account of the observation of the trails of dye which serve to indicate whether the flow near the bed is turbulent or laminar:

(a) Smooth Bottom — By dropping potassium permanganate crystals from the water surface towards the moving bottom, the crystal left a trail of dye in the water. Focusing at a single trail of dye and disregarding the molecular diffusion, one observed that the dye trail was almost straight down to a short distance from the bottom (say in the order of one-quarter inch) and only then began to bend in shape. When the motion of the bottom plate was slow, the trail of dye still maintained a clear line near the bottom. This regular shape of the dye trail became irregular when the speed of the bottom plate was increased to a certain speed, indicating the transition from laminar to turbulent motion. The "bent part" of the dye trail indicated the boundary layer flow. In the laminar layer, the dye trail gave roughly the velocity distribution of the oscillatory boundary layer as given by Equation (15). When the boundary layer, became turbulent, no instantaneous and regular velocity could be traced.

(b) Rough Bottom, half round wooden strips - The observation of the transition from laminar to turbulent flow over the bottom roughened by 1/4", 3/4" and 3/8" half round wooden strips was made in similar way to that over a smooth bottom. Again potassium permanganate crystals were dropped through the water and their dye trails observed. In this case, it was observed that in all cases separation occurred at each roughness element shortly after motion in one direction had started (see figure below).

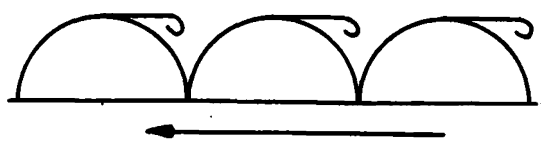

This wake was given during the stroke until the next reversal of motion began

to develop a similar wake on the other side of the strip. As long as these wakes remained permanently in contact with the strips, the flow outside remained perfectly streamlined and was laminar. Whenever the wakes would separate from the strips, they moved into the flow above and created the characteristic mixing effects of turbulent flow. The latter case was called turbulent.

(c) Rough bottom, sand and gravel - The flow patterns near the gravel bed were similar to the descriptions for the half round wooden strips, except that the wake was three-dimensional and the point of separation was not so well defined. The flow patterns near the sand bottom could not be described very well to the smaller scale of motion. But the transition could still be determined by observing the shape of the dye band close to the bottom.

CHAPTER IV

EXPERIMENTAL RESULTS

18. Smooth Bottom

The results of the four different runs with different water depths are plotted in Figure 2 using the total displacement (stroke) d_1, and the $\frac{\omega}{\nu}$ as ordinate and abscissa, respectively. Run 104 (with cross symbol) was observed independently by Dr. Chien, of the Sediment Research Laboratory, University of California. The fact that the results of this observation are not significantly different from those of the other runs indicates that the observations are not significantly affected by personal bias. A line drawn through the experimental points separates the graph into stable and unstable zones; any conditions of the upper right hand zone are unstable and those in the lower left are stable.

Although the experimental points scatter, they seem to follow a straight line of 1 to 2 slope for lower $\frac{\omega}{\nu}$ value (see Figure 2). At higher $\frac{\omega}{\nu}$ values the points begin to deviate from this line.

One may recall that the characteristic Reynolds number for an oscillatory flow over a smooth bed is given by Equation (19).

$$R = \omega^{1/2} d_1 / \nu^{1/2} \tag{19}$$

The fact that experimental points in Figure 2 closely follow a line with a 1 to 2 slope indicates that the transition of the laminar oscillatory flow over a smooth bed takes place at a certain constant Reynolds number. This Reynolds number is found to be 800. One word of caution must be added concerning the definition of smoothness of the boundary. There exists no absolute scale to measure whether a boundary is smooth or rough. A bed which is smooth at low values of $\frac{\omega}{\nu}$ may behave hydraulically rough at higher values of $\frac{\omega}{\nu}$. As with increasing $\frac{\omega}{\nu}$, the boundary layer thickness becomes smaller and approaches the same order of magnitude as the roughness elements. The deviation of the lower part of the experimental data from the straight line may be attributed to the fact that the bed no longer behaves entirely smooth in that range. Furthermore, the elasticity of the steel band at higher value of $\frac{\omega}{\nu}$ causes more distrubances that affect the deviation.

19. Rough Bottom, Two-Dimentional

The results of the experiments using 1-1/4 inch, ; 3/4 inch, 3/8-inch half round and 3/64-inch round rods as roughness elements are shown in Figures 3, 4, 5, and 6, respectively. The difference in the experimental results for the three different sizes of wooden strips is very small and almost within the range of scatter of the experimental data. The line which fits these points assumes a slope close to 1 on 1. At higher values of $\frac{\omega}{\nu}$, the deviation of the experimental data again may be caused by the

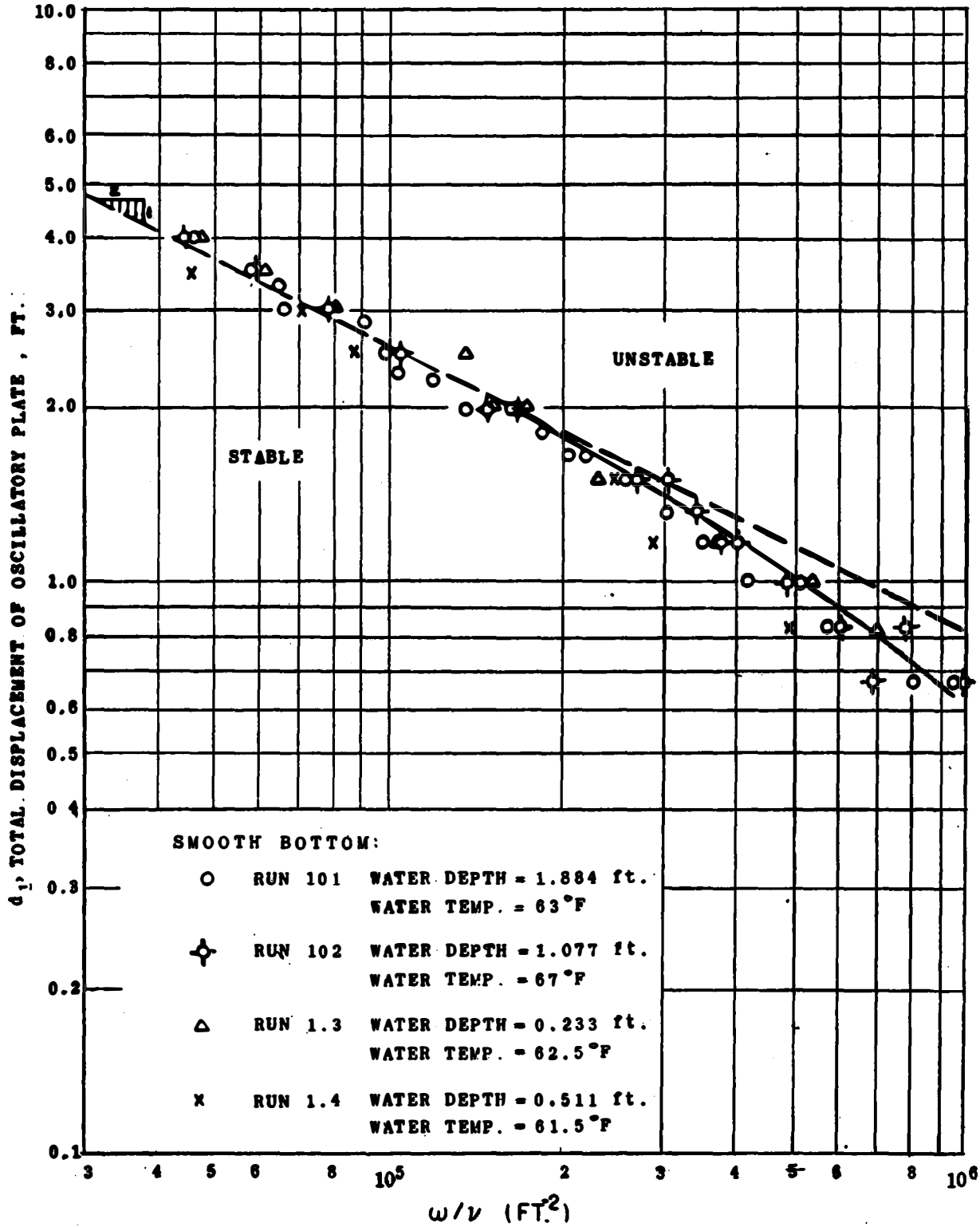

EXPERIMENTAL RESULTS OF TRANSITION INVESTIGATION OF OSCILLATORY MOTION

SMOOTH BOTTOM

FIGURE 2

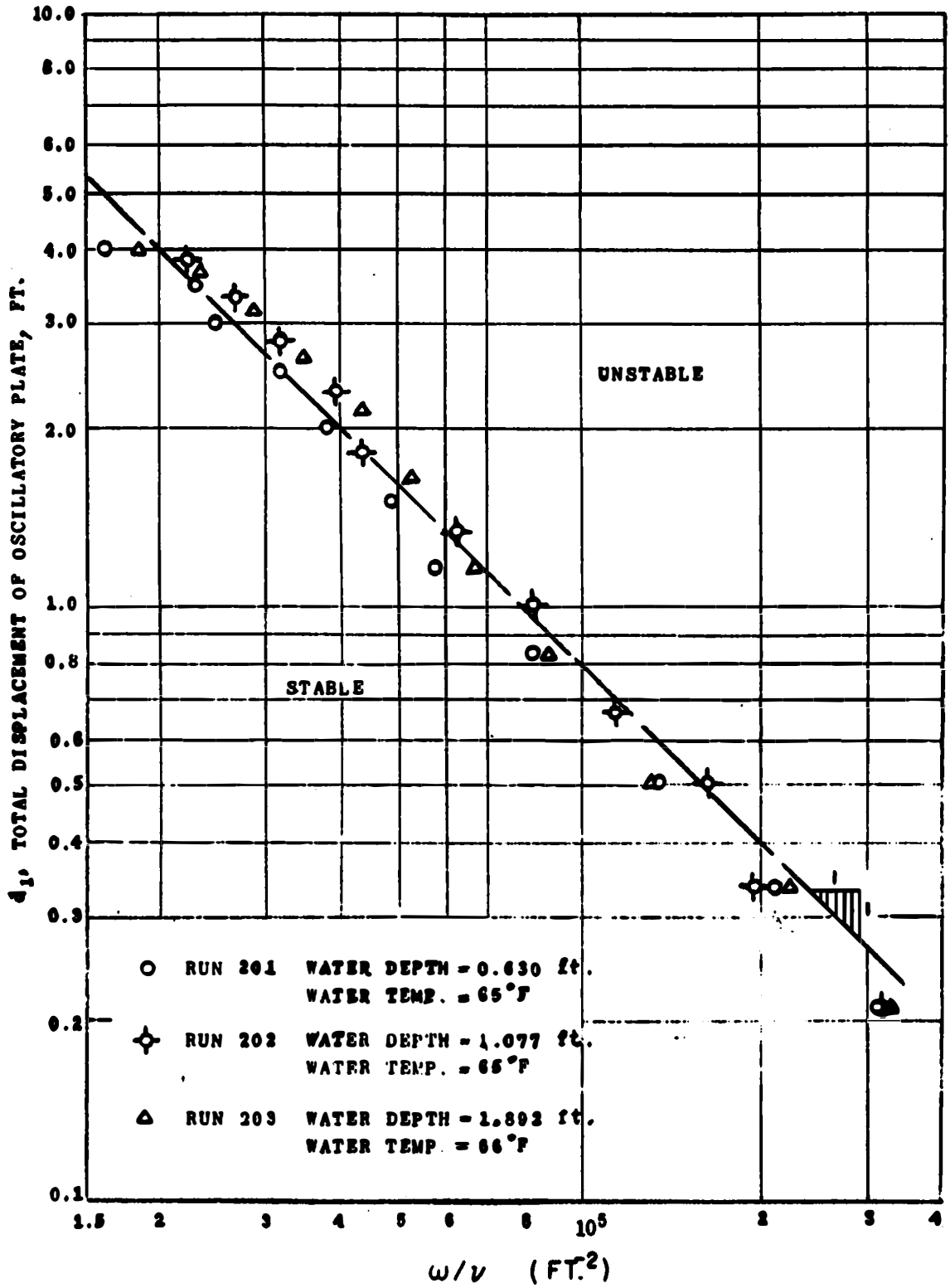

EXPERIMENTAL RESULTS OF TRANSITION INVESTIGATION OF OSCILLATORY MOTION
ROUGH BOTTOM $1\frac{1}{4}$" DIA. HALF ROUND WOODEN STRIPS
FIGURE 3

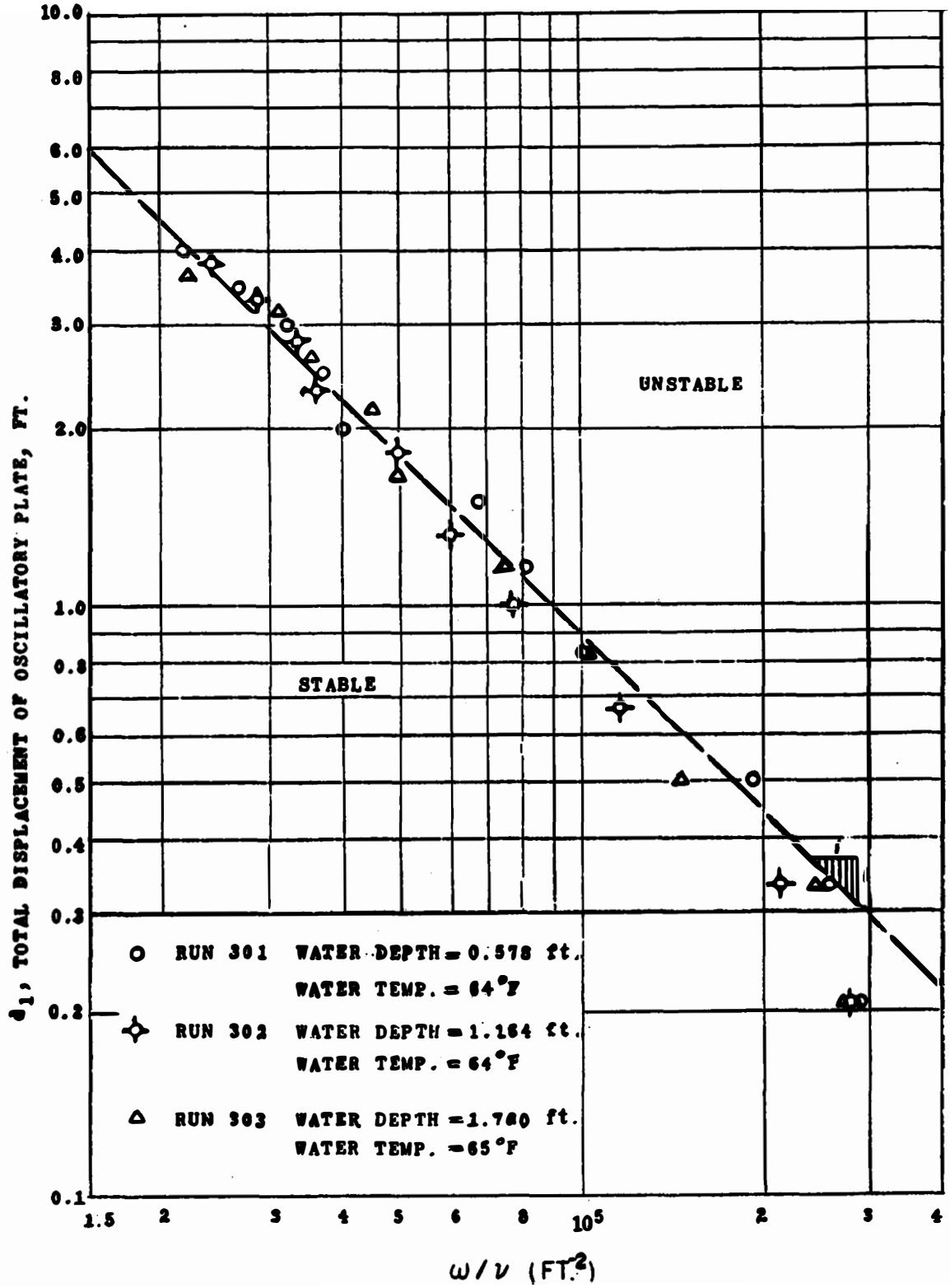

EXPERIMENTAL RESULTS OF TRANSITION INVESTIGATION OF OSCILLATORY MOTION

ROUGH BOTTOM: $\frac{3}{4}$" DIA. HALF ROUND WOODEN STRIPS

FIGURE 4

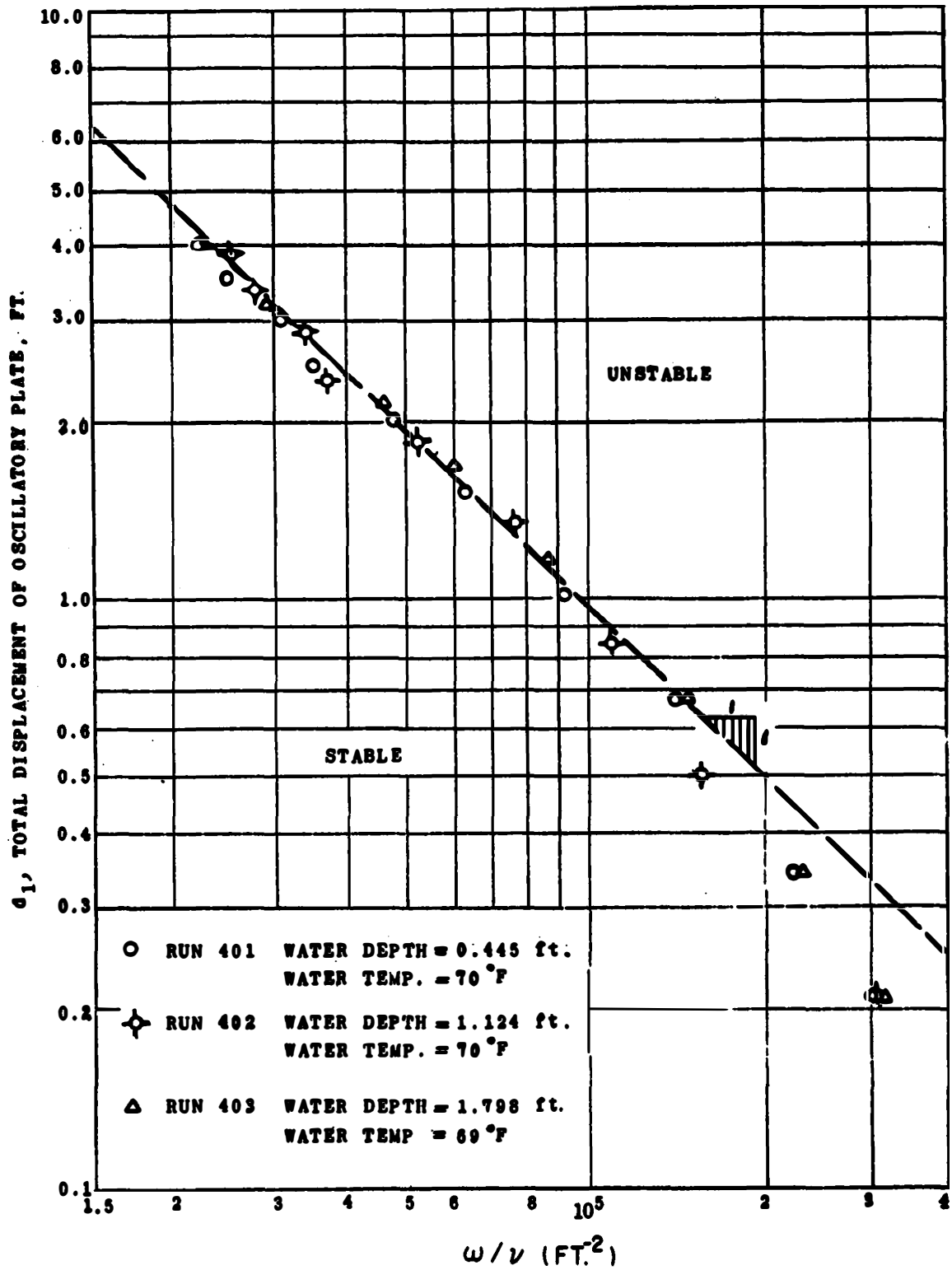

EXPERIMENTAL RESULTS OF TRANSITION INVESTIGATION OF OSCILLATORY MOTION

ROUGH BOTTOM: $\frac{3}{8}$" DIA. HALF ROUND WOODEN STRIPS

FIGURE 5

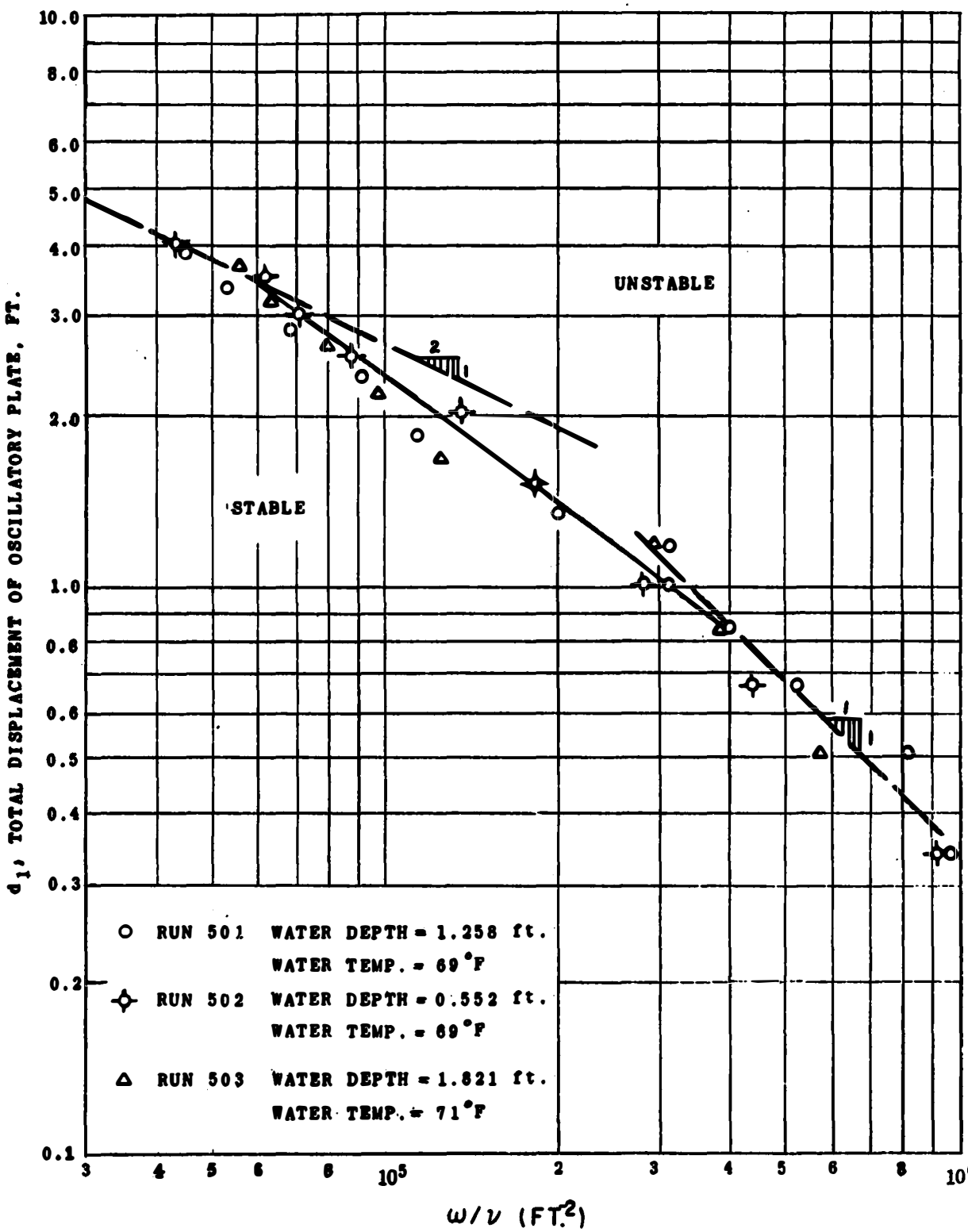

EXPERIMENTAL RESULTS OF TRANSITION INVESTIGATION OF OSCILLATORY MOTION

ROUGH BOTTOM: $\frac{3}{64}$" DIA. HALF ROUND WOODEN STRIPS

FIGURE 6

elasticity of the steel band. This seems to indicate that the transition occurs at a certain constant velocity. The experimental results for the small size 3/64-inch diameter round rods are most interesting. The experimental data follow a straight line with slope 1 on 2 for 4.2×10^4 ft.$^{-2}$ $< \frac{\omega}{\nu} < 6.0 \times 10^4$ ft.$^{-2}$. After a gradual transition, the points follow another straight line with a slope 1 to 1 for 4×10^5 ft.$^{-2} < \frac{\omega}{\nu} < 1.0 \times 10^6$ ft.$^{-2}$. That is, those rods behave hydraulically smooth at low $\frac{\omega}{\nu}$ values and become rough at high $\frac{\omega}{\nu}$ values. This is to be expected, as at low $\frac{\omega}{\nu}$ the boundary layer thickness is so large that it practically covers the roughness elements.

20. Rough Bottom, Three-Dimensional

The experimental results for the sand and gravel bottom are presented in Figures 7, 8, 9, and 10. Straight lines with a 1 to 1 slope seem to fit the data fairly well for these cases, except at low $\frac{\omega}{\nu}$ values for the 0.0009-ft. sand.

A comparison of the results for two-dimensional and three-dimensional roughnesses indicates that the gravel bottom behaves very similar to the bottom with half round wooden strips while the sand and the polystyrene pellet behave somewhat differently. The experimental data for the sand bottom shift to the right, indicating that the flow is more stable but not as stable as the results with round steel rods. Actually, the sand size is smaller than the diameter of the steel rod; the transition may be due to the different flow patterns around the sand and the steel rod. In fact, the "effective roughnesses" are different in the two cases.

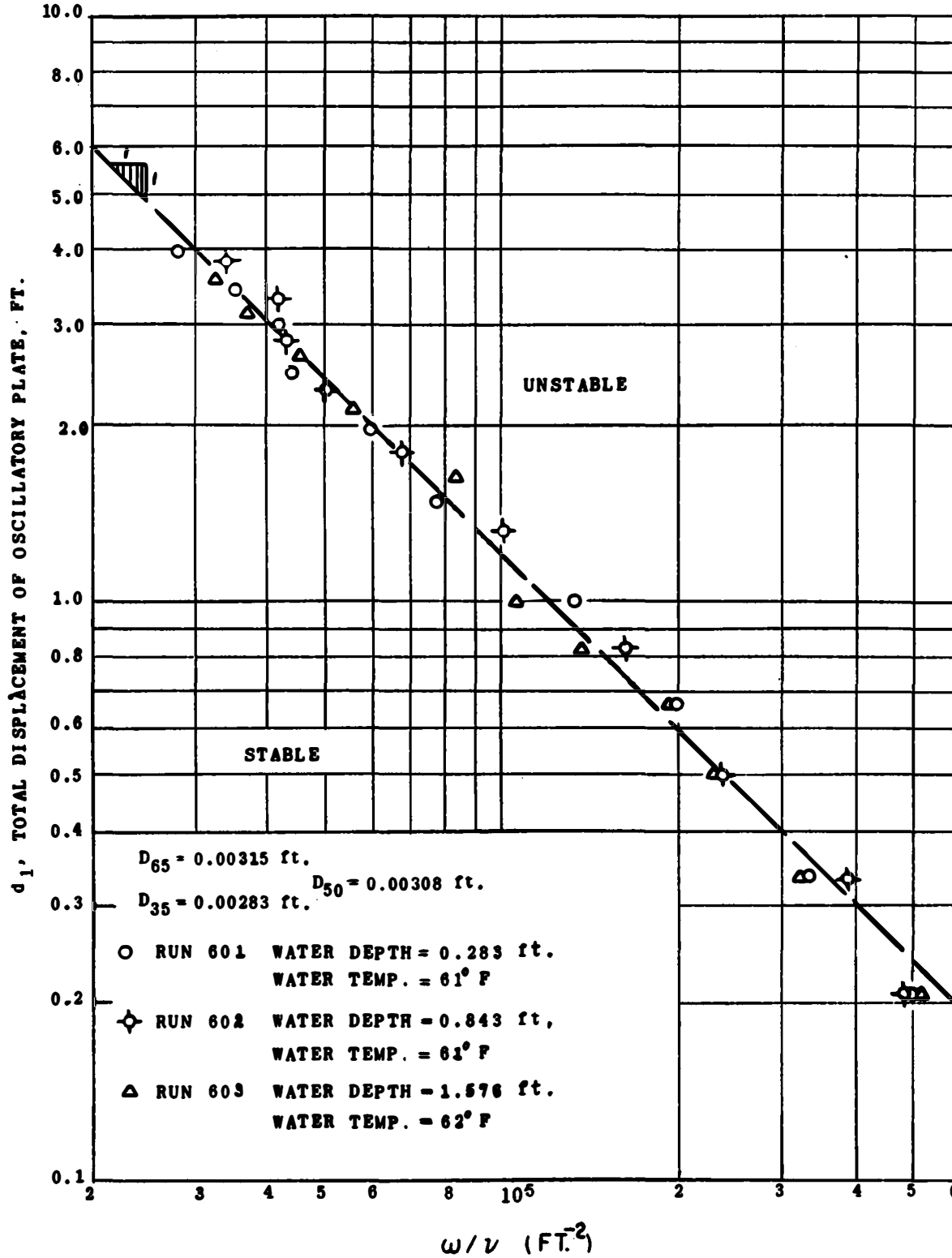

EXPERIMENTAL RESULTS OF TRANSITION INVESTIGATION OF OSCILLATORY MOTION
ROUGH BOTTOM: MEAN SAND SIZE = 0.00308 ft.
FIGURE 7

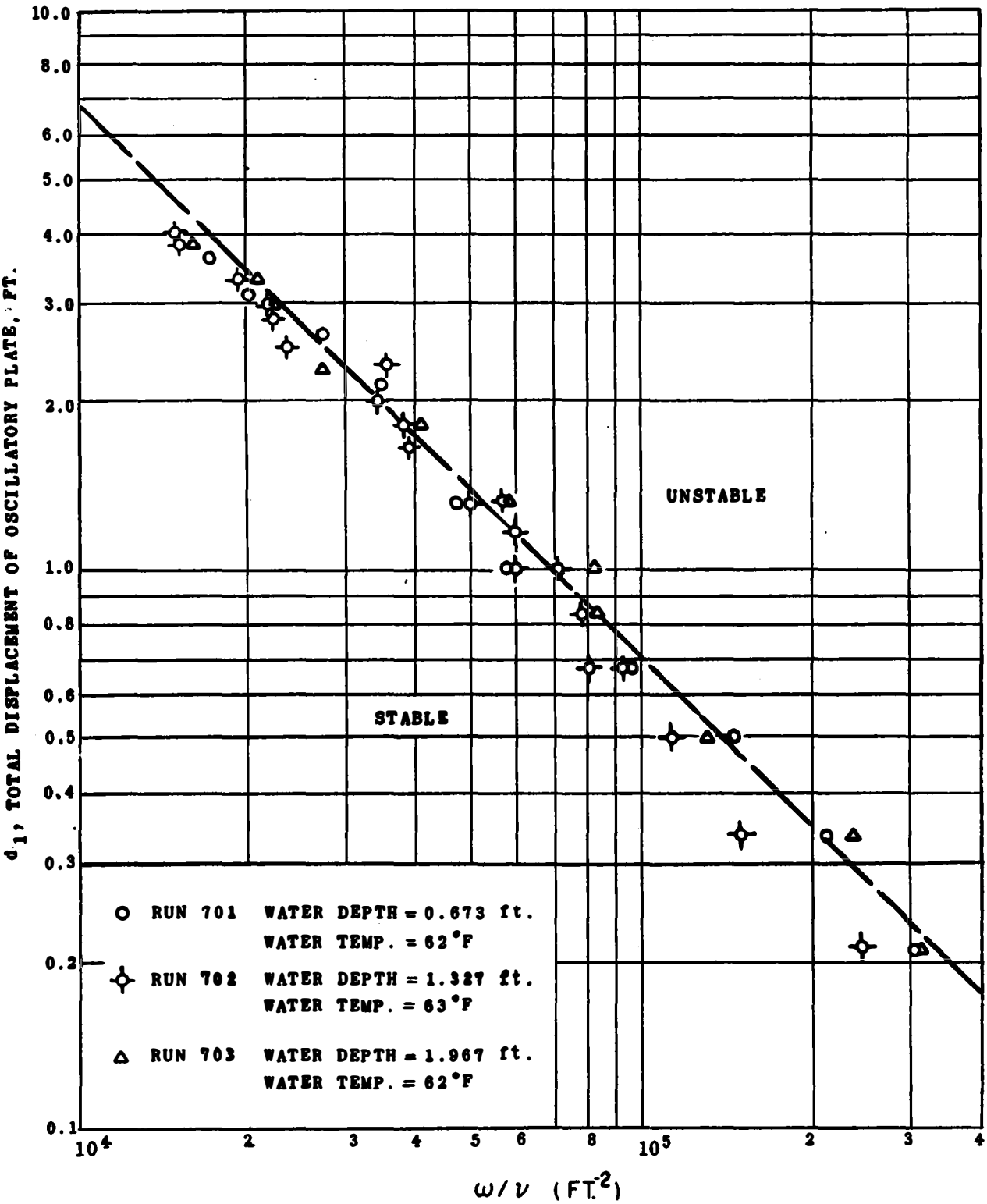

EXPERIMENTAL RESULTS OF TRANSITION INVESTIGATION OF OSCILLATORY MOTION

ROUGH BOTTOM: GRAVEL SIZE = 0.0453 ft.

FIGURE 8

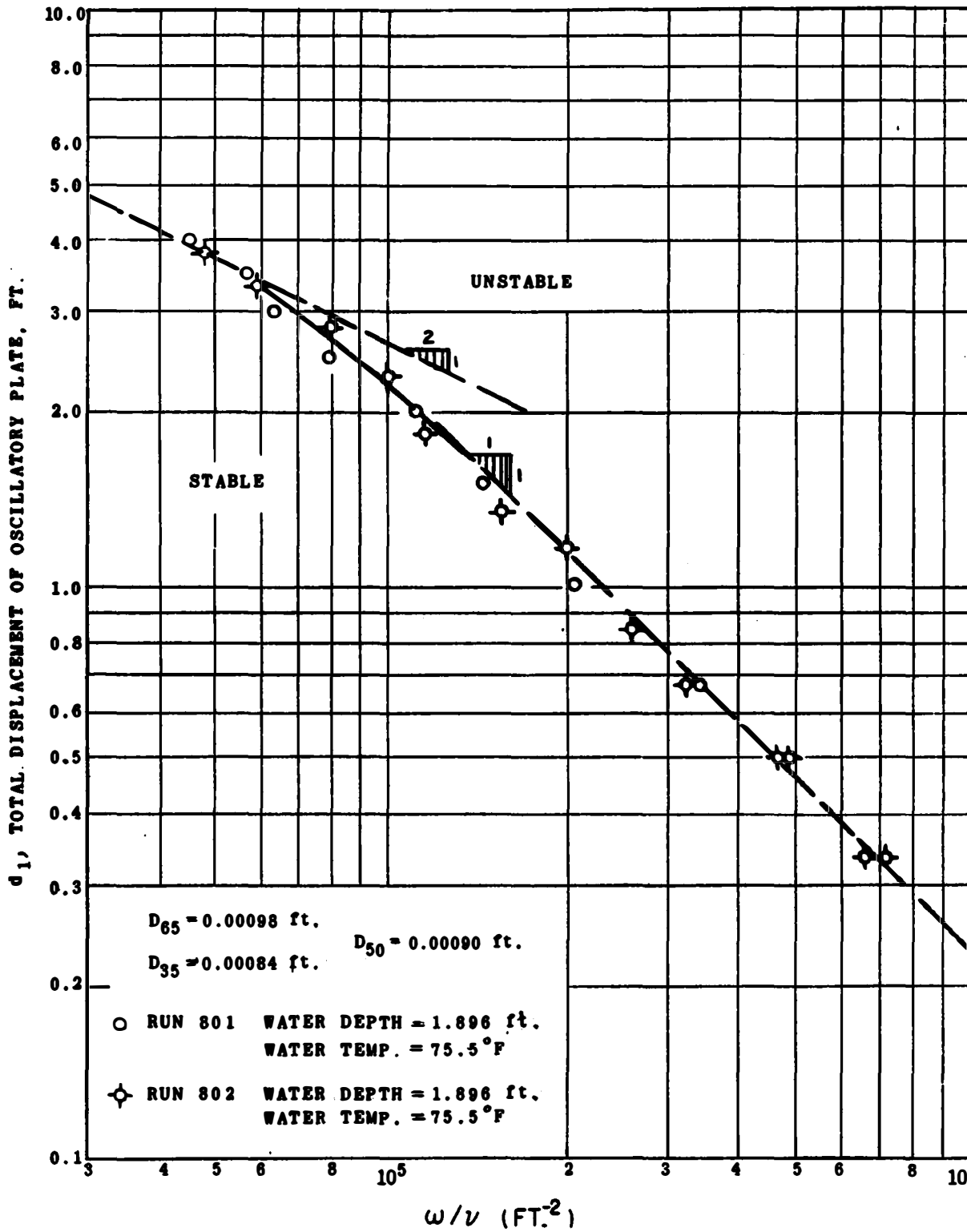

EXPERIMENTAL RESULTS OF TRANSITION INVESTIGATION OF OSCILLATORY MOTION
ROUGH BOTTOM: SAND SIZE = 0.00090 ft.

FIGURE 9

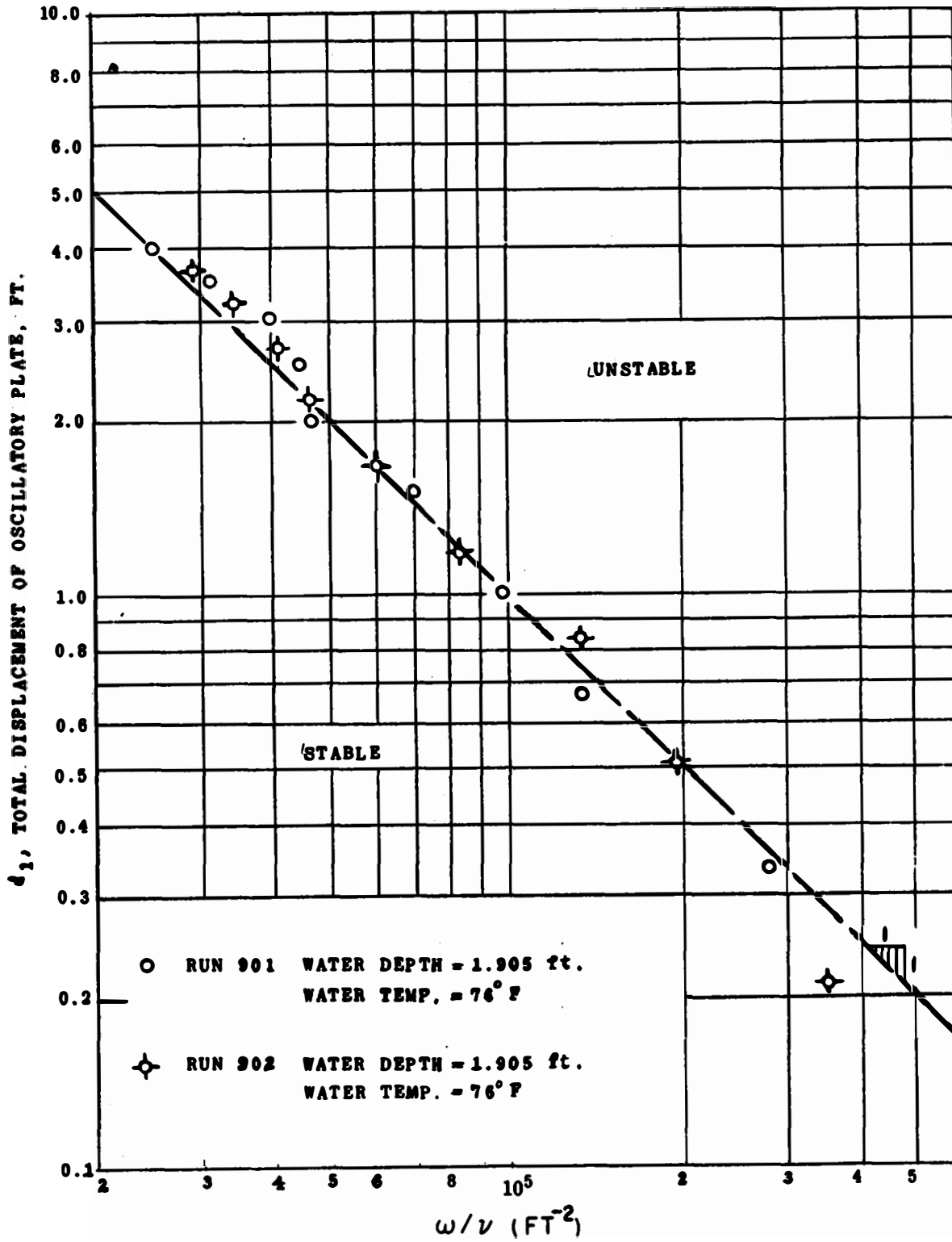

EXPERIMENTAL RESULTS OF TRANSITION INVESTIGATION OF OSCILLATORY MOTION
ROUGH BOTTOM: POLYSTRENE PELLETS SIZE = 0.0104 ft
FIGURE 10

CHAPTER V

DISCUSSION OF THE EXPERIMENTAL RESULTS

21. Limitation of the Experiments

The experiments as described in the preceding chapter are carried out in a range where the stroke d_1 is larger than the roughness diameter ϵ. The flow condition in the boundary layer may become somewhat different if d_1 is of the same order or smaller than ϵ. In that case the oscillatory motion is limited to the neighborhood of an individual roughness element, and the latter may have no effect on the transition. Or in other words, the bed may behave hydraulically smooth when $d_1 << \epsilon$. This case is not studied in the investigation because of its lack of practical significance.

22. On the Length Scales

In finding a parameter which will describe the transition of an oscillatory flow, difficulty arises when one attempts to select a suitable length scale. The experimental results indicate that the water depth does not come into the picture so long as it is much larger than the thickness of the boundary layer flow. For certain water depths and frequencies of oscillation, standing waves are generated in the flume. Yet, they are of such small magnitude in comparison with the main motion that they seem to have no apparent effect on the results. The total displacement or stroke of the oscillation is a well defined length scale, and the ratio $\frac{d_1}{\epsilon}$ has significance as depicted before. However, under ordinary conditions when d_1 is much larger than the roughness diameter, it does not seem to be significant as a length scale. One should expect that the boundary layer thickness and the roughness diameter are more significant.

23. On the Smooth Bottom

For a smooth bottom the experimental results indicate that the critical Reynolds number (defined by Equation 19) of the transition can be used to define the critical condition and that it has a value of 800. This is also true for the 3/64-inch diameter steel rods (Figure 6) and 0.0009-ft. diameter sand bottom (Figure 9) at very low speed. The smooth bottom is defined as follows:

1. For a smooth bottom the roughness is small compared with the laminar boundary layer thickness (See Section 25).

2. For a smooth bottom the presence of roughness, although it created small finite disturbances, does not change the flow pattern of the basic flow.

24. On the Rough Bottom

According to the experimental results, the critical Reynolds number $\frac{\omega d_1 \epsilon}{\nu}$ of the transition has a constant value for each roughness, but

this value changes with ϵ. The effects of roughness have been described in Section 8 and the flow pattern is shown in Section 17. It is not surprising that the critical Reynolds number is not a constant for all roughness. The transition from laminar flow to turbulence at the rough bottom is mainly due to the instability of the flow along the wakes between the individual roughness elements.

The experimental results in terms of $\frac{\omega d_1 \epsilon}{\nu}$ against $\frac{\omega^{1/2} d_1}{\nu^{1/2}}$ are presented in Figures 11 and 12, with ϵ as a parameter for two and three-dimensional roughness, respectively, (where ϵ = diameter of the half round wooden strips and the diameter of the round steel rods, ϵ = average size of the sand and gravel). The vertical line $\frac{\omega^{1/2} d_1}{\nu^{1/2}} = 800$ represents a smooth surface with a constant Reynolds number of the form $\frac{\omega^{1/2} d_1}{\nu^{1/2}}$. The horizontal lines represent the rough walls. A transition zone seems to exist between the smooth and rough boundaries.

25. Classification of the Smooth and Rough Boundaries

From the experimental results of the 3/64-inch round steel rods bottom (Figure 6) and the 0.0009-ft. diameter sand bottom (Figure 9) the smooth and rough boundaries can be classified as follows:

1. Two-dimensional roughness

   a. Smooth boundary exists if

   $$\frac{\delta_1}{\epsilon} = \frac{6.5\sqrt{\frac{\nu}{\omega}}}{\epsilon} > \frac{6.5\sqrt{\frac{1}{6 \times 10^4}}}{0.0039} = 6.8$$

   b. Rough boundary exists if

   $$\frac{\delta_1}{\epsilon} = \frac{6.5\sqrt{\frac{\nu}{\omega}}}{\epsilon} < \frac{6.5\sqrt{\frac{1}{4 \times 10^6}}}{\epsilon} = 2.6$$

   c. Transition from smooth to rough boundary

   $$6.8 > \frac{6.5\sqrt{\frac{\nu}{\omega}}}{\epsilon} > 2.6$$

2. Three-dimensional roughness

   a. Smooth boundary exists if

   $$\frac{\delta_1}{\epsilon} = \frac{6.5\sqrt{\frac{\nu}{\omega}}}{\epsilon} > \frac{6.5\sqrt{\frac{1}{6 \times 10^4}}}{0.0009} = 30$$

   b. Rough boundary exists if

   $$\frac{\delta_1}{\epsilon} = \frac{6.5\sqrt{\frac{\nu}{\omega}}}{\epsilon} < \frac{6.5\sqrt{\frac{1}{1.5 \times 10^6}}}{0.0009} = 18.5$$

   c. Transition from smooth to rough boundary

   $$30 > \frac{6.5\sqrt{\frac{\nu}{\omega}}}{\epsilon} > 18.5$$

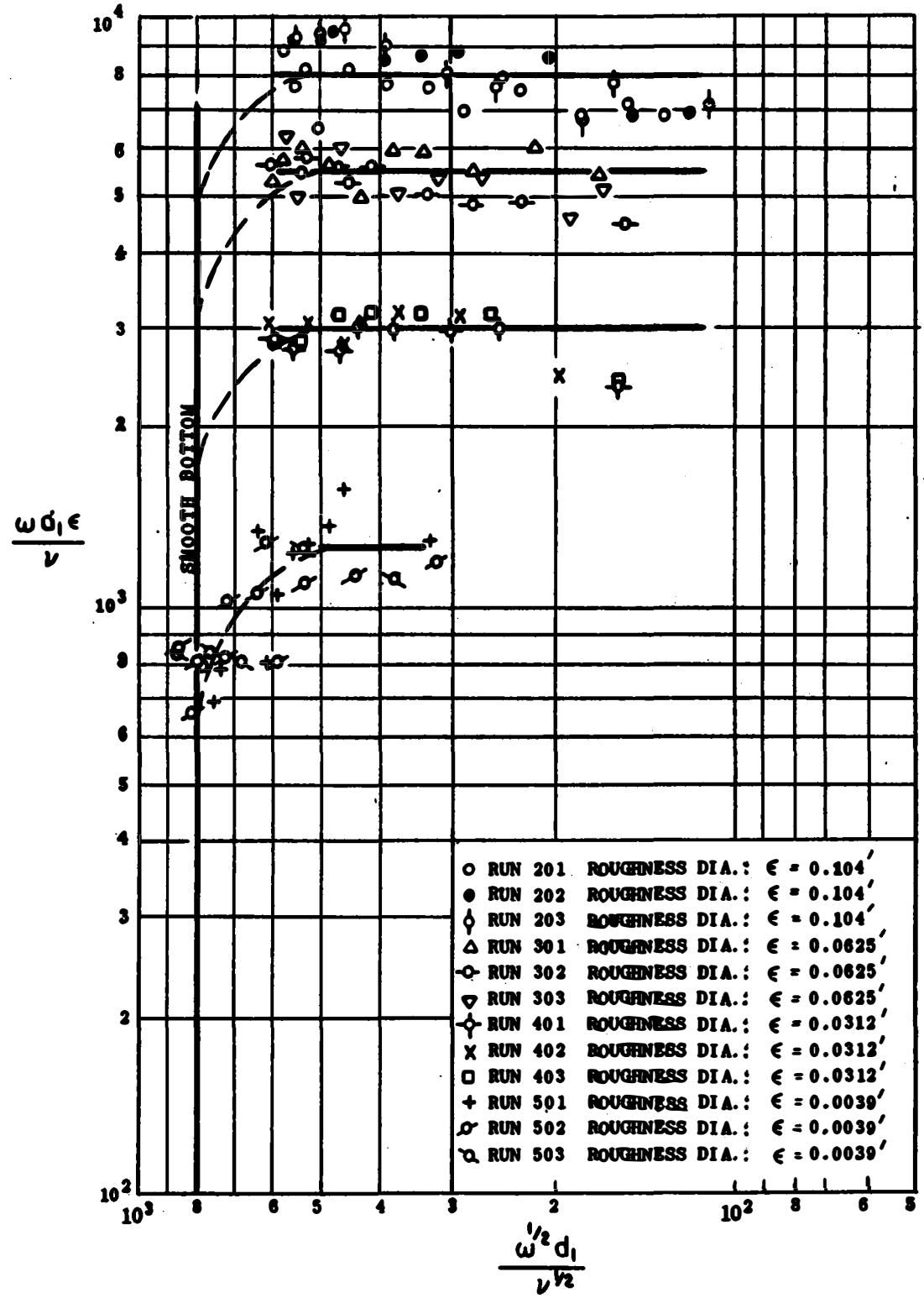

PLOT OF EXPERIMENTAL RESULTS IN TERMS OF $\frac{\omega d_1 \epsilon}{\nu}$ VS $\frac{\omega^{1/2} d_1}{\nu^{1/2}}$

ROUGH BOTTOM: HALF ROUND WOODEN STRIPS AND ROUND STEEL RODS

(TWO DIMENSIONAL)

FIGURE 11

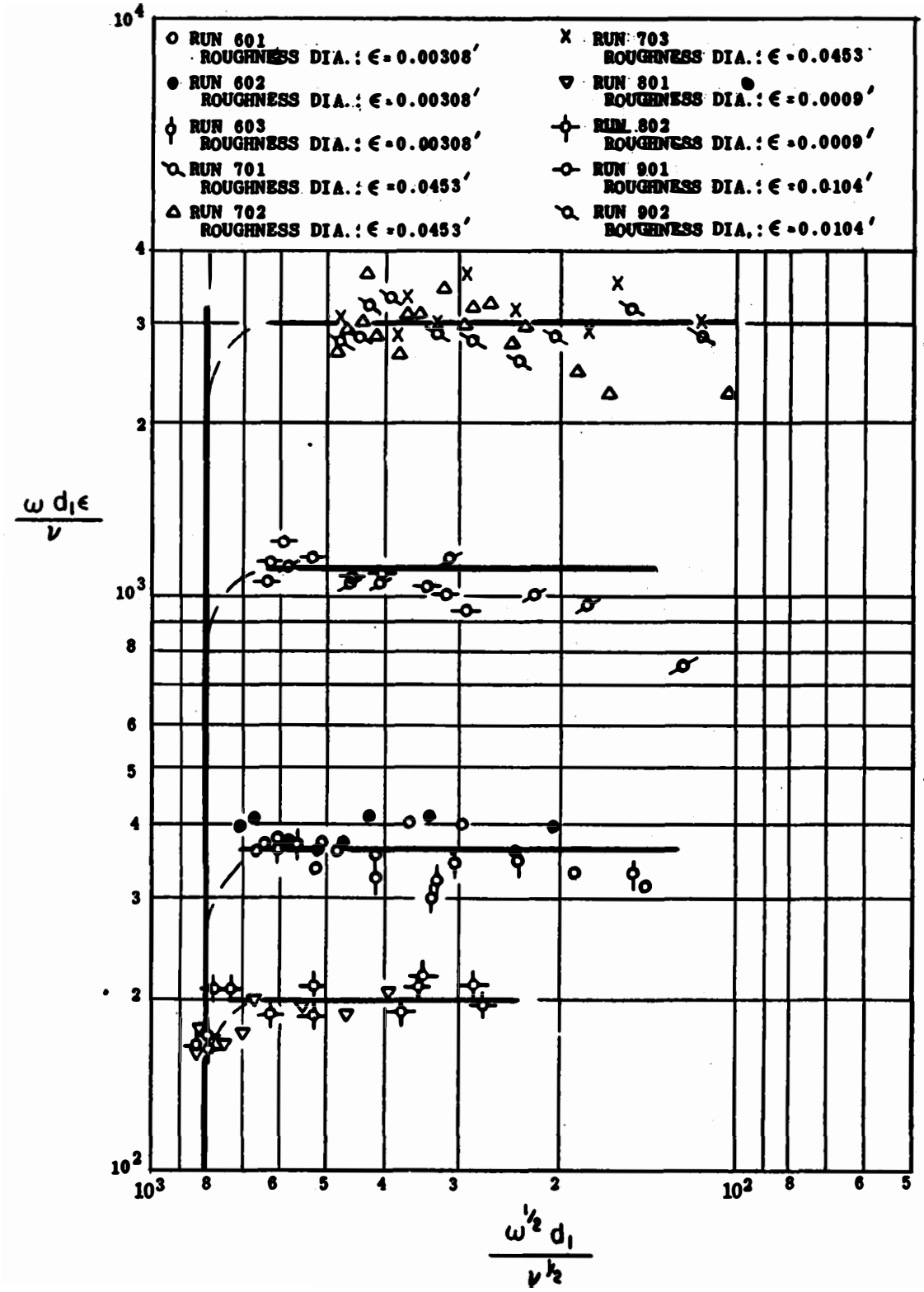

PLOT OF EXPERIMENTAL RESULTS IN TERMS OF $\frac{\omega d_1 \epsilon}{\nu^{1/2}}$ VS $\frac{\omega^{1/2} d_1}{\nu^{1/2}}$

ROUGH BOTTOM: SAND AND GRAVEL (THREE DIMENSIONAL)

FIGURE 12

26. Notes on the Experiment

Turbulence is a random motion with characteristic mixing. This is the criterion for the visual determination of the transition. For the smooth bed, the trails of dye follow the oscillatory motion near the bottom and remain continuous when the flow is laminar. Although molecular diffusion exists, there is definitely no random mixing. As the frequency of the oscillation increases up to a certain limit, the regular motion of the dye breaks down, and the trail of dye cannot be recognized any more. However, the transition between the laminar and turbulent motion is not sharply defined. This is the main reason for the scatter of the experimental data. Over a rough bottom the trail of dye is somewhat different (See Section 17). Even in the laminar range wakes are present. The pattern of these wakes is rather regular and should not be regarded as turbulent motion.

27. Suggestions for Further Investigation

Two possible ways of approach are suggested to study theoretically the stability of the oscillatory boundary layer flow for smooth case: (1) by superimposing the infinitesimal disturbances to the linearized oscillatory boundary layer equation, (2) by retaining the nonlinear terms in the equation of motion. It seems that the first method will lead to great mathematical difficulties, because both the oscillatory flow and the disturbances are functions of time. It may be possible to get the solution by assuming that the frequency of the oscillatory flow is much lower than the frequency of the disturbance. The second method is very possible to give usable results.

The present experimental study may be improved by:

1. Increasing the length of the oscillatory plate as well as the length of the flume to eliminate the end effects.

2. Improving the steel band (either make it tighter, or use stiff material) to eliminate the elastic effects.

3. Using heavy surface floats to eliminate the standing wave.

In order to study the viscosity effect, experiments with fluids of different viscosity are suggested.

CHAPTER VI

CONCLUSIONS

The transition from laminar to turbulent flow in an oscillatory flow near both smooth and rough boundaries has been studied. The findings of this investigation are summarized as follows:

(1) Over a smooth boundary, the critical Reynolds number at which the transition takes place is found to be a constant

$$R = \omega^{1/2} d_1 / \nu^{1/2} = 800$$

In this case the boundary layer thickness is taken as the characteristic length scale.

(2) For a rough boundary, the critical Reynolds number has the form $\frac{\omega d_1 \epsilon}{\nu} = C$ and is a constant for each roughness. No single parameter of transition has been found for similar rough boundaries.

(3) Wakes have been observed to develop behind each roughness element for the oscillatory flow over a rough bottom. The transition from laminar flow to turbulent is mainly due to instability of the flow along these wakes.

(4) The effect of two-dimensional roughness, using half cylinders as roughness elements, is different from that of three-dimensional roughness where the bed consisted of sand and gravel. The flow is more stable over the former than over the latter for the same roughness size.

(5) Based on the experimental results of the 3/64-inch round steel rods bottom and 0.0009-ft. diameter sand bottom, the bed behaves hydraulically rough if

$$\frac{\delta_1}{\epsilon} = \frac{6.5\sqrt{\frac{\nu}{\omega}}}{\epsilon} < 2.6 \qquad \text{for two-dimensional roughness}$$

$$\frac{\delta_1}{\epsilon} = \frac{6.5\sqrt{\frac{\nu}{\omega}}}{\epsilon} < 18.5 \qquad \text{for three-dimensional roughness}$$

The bed behaves hydraulically smooth if

$$\frac{\delta_1}{\epsilon} = \frac{6.5\sqrt{\frac{\nu}{\omega}}}{\epsilon} > 6.8 \qquad \text{for two-dimensional roughness}$$

$$\frac{\delta_1}{\epsilon} = \frac{6.5\sqrt{\frac{\nu}{\omega}}}{\epsilon} > 30 \qquad \text{for three-dimensional roughness}$$

(6) The flow pattern is expected to be different for $\frac{\epsilon}{d_1} < 1$ and $\epsilon/d_1 > 1$; the experimentation for this study was confined to the case $\epsilon/d_1 < 1$ which has more practical applications.

ACKNOWLEDGMENTS

The author wishes to express his appreciation for the advice and encouragement of Professor H. A. Einstein, under whose direction this work was carried out, and for the valuable criticism and discussion of Professor J.W. Johnson and P. L. Chambré. The cooperation and assistance of the staff of the Fluid Mechanics Laboratory is here gratefully acknowledged. The writer also wishes to thank Dr. Ning Chien of the Sediment Research Laboratory of the University of California for his assistance in the study and careful examination of the manuscript.

REFERENCES

1. Reynolds, O., "An Experimental Investigation of the Circumstances which Determine Whether the Motion of Water Shall be Direct or Sinnous and of the Laws of Resistance", Phil. Tran. Roy. Soc. London, Vol. 174, Part 3, 1883, p. 935.

2. Kelvin, L., "Mathematical and Physical Papers", Cambridge Univ. Press, Vol. 4, 1887, p. 321

3. Prandtl, L., "Neuere Ergebnisse der Turbulenztorschung", Zeitschrift des Vereines Deutscher Ingenieure, Bd. 77, No. 5, 1933, p. 105

4. Tollmien, W., "Ueber die Entstehung der 'Turbulenz'", Nachr. Cres. Wiss. Göttingen Math. Phy. Klasse, 1929, p. 21.

5. Schlichting, H., "Lecture Series 'Boundary Layer Theory'", Part II - Turbulent Flows", NACA T. M. No. 1218, 1949.

6. Lin, L. L., "On The Stability of Two-Dimensional Parallel Flows", Quarterly of Applied Mathematics, Vol. III, No. 2, 1945, p. 117; Vol. II, No. 3, 1946, p. 219, Vol. III, No. 4, 1946,p. 277.

7. Reynolds, O. "On the Dynamical Theory of Incompressible Viscous Fluid, and the Determination of the Criterion", Phil. Trans. Roy. Soc. London, (A) Vol. 186, Part 1, 1895, p. 123.

8. Schiller, L., "Strömungsbilder zer Entstehung der Turbulenten Rohrströmung", Proc. Third Int. Cong. Appl. Mech., Vol. 1, 1931, Stockholm, p. 226.

9. Taylor, G. I., "Some Recent Developments in the Study of Turbulence", Proc. Fifth Int. Cong. Appl. Mech., 1938, Cambridge, Mass., p. 294.

10. Rayleigh, L., "Propagation of Waves upon Plane Surfaces Separating Two Portions of Fluid of Different Vorticities", Proc. London Math. Soc., Vol. 10, 1879; p. 4-13, Vol. 11, 1880, p. 47-70; Vol. 19, 1887, p.67-74; Vol. 27, 1895, p. 5-12.

11. Taylor, G. I., "Stability of Viscous Liquid Contained Between Two Rotating Cylinders", Phil. Trans. Roy. Soc., London (A) 223, 1923, p. 289.

12. Lewis, J. W., "An Experimental Study of Motion of a Viscous Liquid Contained Between Two Coaxial Cylinders", Proc. Roy. Soc., London, (A) 118, 1928, p. 388.

13. Schlichting, H., "Zur Entstehung der Turbulenz bei der Plattenströmung", Nachrichten Gesellschaft der Wissenschaft zu Göttingen Mathemathische - Physikaliche Klasse, 1933, p. 181-208.

14. Schlichting, H., "Amplitudenventeilung und Energiebilanz der Kleinen Storungen bei der Plattenströmung", Nachr. Gen. Wiss. Gottingen Math. Phy. Klasse, Vol..1, 1935, p. 47.

15. Lees, L., "The Instability of the Laminar Boundary Layer in a Compressible Fluid", NACA T. N. 1360, July 1947.

16. Dunn, D. W. and Lin, C. C., "On Stability of the Laminar Boundary Layer in a Compressible Fluid, Part I", Report, Department of Mathematics, M.I.T., December, 1953.

17. Lessen, M., "On Stability of Free Laminar Boundary Layer Between Parallel Streams", NACA Annual Report No. 979, 1950, p. 571.

18. Schubauer, B. and Skramstad, H. K., "Laminar Boundary Layer Oscillations and Transition on a Flat Plate", Journal of Research, U. S. Bureau of Standards, 1947, p. 251.

19. Liepmann, H. W., "Investigation of Laminar Boundary Layer Stability and Transition on Curved Boundary", NACA ACR 3H 30, August 1943 (NACA Wartime Report W-107).

20. Emmons, H. W., "The Laminar-Turbulent Transition in a Boundary Layer", Part I, Jour. Aero. Sci., Vol. 18, No. 7, p. 490, July 1951.

21. Dryden, H. L., "Review of Published Data on the Effect of Roughness on Transition from Laminar to Turbulent Flow", Journ. of Aero. Sci., Vol. 20, No. 7, p. 477, July 1953.

22. Hama, F. R. and Tani, I., "Some Experiments on the Effect of a Single Roughness Element on Boundary Layer Transition", Jour. Aero. Sci., Vol. 20, No. 4, p. 289, April 1953.

23. Wiegel, R. L. and Johnson, J. W., "Elements of Wave Theory", Coastal Engineering, October 1950.

Appendix

Experimental Data and Tables of Calculation

I. Smooth Bottom

TABLE I

Run No. 101
Water depth: 1.884 ft.
Water temp.: 63°F
Kinematic viscosity: $\gamma = 1.15 \times 10^{-5}$ ft.²/sec.

cpm	Total Displacement d_1 ft	Angular Velocity ω rad/sec	$\frac{\omega}{\gamma}$ $\frac{1}{ft^2}$	$\frac{\omega^{\frac{1}{2}} d_1}{\gamma^{\frac{1}{2}}}$
28.0	1.50	2.93	2.55×10^5	757
34.5	1.333	3.61	3.05	735
38.5	1.167	4.03	3.51	688
46.1	1.00	4.82	4.17	645
63.8	0.833	6.68	5.80	633
104.0	0.667	10.9	9.53	650
18.0	2.000	1.88	1.64	810
20.3	1.833	2.13	1.85	782
22.7	1.667	2.38	2.07	757
24.2	1.667	2.53	2.20	777
57.1	1.0	5.98	5.2×10^5	713
90.0	0.667	9.42	8.18	601
5.07	4.00	0.53	0.462	857
6.36	3.5	0.665	0.578	840
7.34	3.0	0.767	0.666	772
10.9	2.5	1.14	0.99	780
13.0	2.333	1.36	1.18	800
15.0	2.167	1.57	1.36	798
16.8	2.00	1.76	1.53	777
7.11	3.333	0.744	0.647	840
9.9	2.833	1.04	0.905	850
11.5	2.333	1.21	1.045×10^5	755

TABLE II

Run No. 102
Water depth: 1.077 ft. Water temp.: 67° F
Kinematic Viscosity: $\gamma = 1.08 \times 10^{-5}$ ft²/sec.

cpm	Total Displacement d_1 ft.	Angular Velocity ω rad/sec	$\frac{\omega}{\gamma}$ $\frac{1}{ft^2}$	$\frac{\omega^{\frac{1}{2}} d_1}{\gamma^{\frac{1}{2}}}$
4.56	4.0	0.477	0.441×10^5	840
6.02	3.5	0.628	0.582	842
8.25	3.0	0.862	0.798	847
10.8	2.5	1.13	1.045	806
15.4	2.0	1.61	1.49	772
31.6	1.5	3.30	3.05	827
35.3	1.333	3.69	3.42	780
41.7	1.167	4.35	4.02	738
50.9	1.00	5.32	4.92×10^5	700
58.8	0.833	6.15	5.70	628
72.3	0.667	7.52	6.97	557
17.3	2.0	1.81	1.68	820
27.8	1.5	2.91	2.70	778
40.0	1.167	4.18	3.87	727
82.0	0.833	8.57	7.92	740
105.0	0.667	10.95	10.1×10^5	668

TABLE III

Run No. 103
Water depth: 0.233 ft. Water temp.: 62.5° F
Kinematic Viscosity: $\gamma = 1.16 \times 10^{-5}$ ft²/sec.

cpm	Total Displacement d_1 ft	Angular Velocity ω rad/sec	$\frac{\omega}{\gamma}$ $\frac{1}{ft^2}$	$\frac{\omega^{\frac{1}{2}} d_1}{\gamma^{\frac{1}{2}}}$
17.0	2.0	1.77	1.52×10^5	780
25.7	1.5	2.68	2.31	720
33.3	1.333	3.48	3.0	730
41.4	1.167	4.32	3.73	713
60.6	1.00	6.33	5.47	738
78.0	0.833	8.13	7.02	698
108.0	0.667	1.13	9.76×10^5	658
5.33	4.0	0.557	0.48	875
6.8	3.5	0.71	0.612	865
9.0	3.0	0.94	0.81	852
15.0	2.5	1.57	1.35	917
19.3	2.0	2.01	1.73×10^5	895

TABLE IV

Run No. 104
Water depth: 0.511 ft. Water temp.: 61.5° F
Kinematic Viscosity: $\gamma = 1.18 \times 10^{-5}$ ft²/sec.

cpm	Total Displacement d_1 ft	Angular Velocity ω rad/sec.	$\frac{\omega}{\gamma}$ $\frac{1}{ft^2}$	$\frac{\omega^{\frac{1}{2}} d_1}{\gamma^{\frac{1}{2}}}$
5.20	3.5	0.543	0.461×10^5	750
8.18	3.0	0.855	0.724	808
9.27	2.5	0.97	0.822	715
28.1	1.5	2.94	2.49	747
32.6	1.167	3.41	2.89	627
56.1	0.833	5.87	4.97×10^5	587

II. Rough Bottom - half round wooden strips and round steel rods

TABLE V

Run No. 201
$1\frac{1}{4}$" dia. half round wooden strips $\epsilon = 0.104$ ft.
Water depth: 0.630 ft. Water temp.: 65° F
Kinematic Viscosity: $\gamma = 1.1 \times 10^{-5}$ ft²/sec.

cpm	Total Displacement d_1 ft	Angular Velocity ω rad/sec	$\frac{\omega}{\gamma}$ $\frac{1}{ft^2}$	$\frac{\omega^{\frac{1}{2}} d_1}{\gamma^{\frac{1}{2}}}$	$\frac{\omega d_1 \epsilon}{\gamma}$
1.66	4.0	0.174	0.158×10^5	502	6.57×10^3
2.38	3.5	0.249	0.226	526	8.22
2.55	3.0	0.267	0.243	468	7.52
3.30	2.5	0.345	0.313	442	8.13
2.98	2.0	0.412	0.374×10^5	387	7.78×10^3
5.07	1.5	0.530	0.482	329	7.52
6.00	1.167	0.628	0.572	278	6.93
8.70	0.833	0.910	0.827	239	7.54
14.0	0.500	1.46	1.325	182	6.89
21.7	0.333	2.27	2.06	151	7.13
32.6	0.208	3.41	3.1×10^5	116	6.7×10^3

TABLE VI

Run No. 202
$1\frac{1}{4}$" dia. half round wooden strips $\epsilon = 0.104$ ft.
Water depth: 1.077 ft. Water temp.: 65°F
Kinematic Viscosity: $\gamma = 1.1 \times 10^{-5}$ ft.²/sec.

cpm	Total Displacement d_1 ft.	Angular Velocity ω rad./sec.	$\frac{\omega}{\gamma}$ $\frac{1}{ft.^2}$	$\frac{\omega^{\frac{1}{2}} d_1}{\gamma^{\frac{1}{2}}}$	$\frac{\omega d_1 \epsilon}{\gamma}$
2.31	3.833	0.242	0.22×10^5	567	8.78×10^3
2.80	3.333	0.293	0.266	542	9.22
3.28	2.833	0.343	0.311	498	9.18
4.09	2.333	0.428	0.391	461	9.47
4.58	1.833	0.480	0.436	382	8.32
6.56	1.333	0.686	0.623	332	8.63
8.75	1.00	0.915	0.832	288	8.63
12.0	0.667	1.255	1.14	246	7.90
17.1	0.500	1.79	1.625	201	8.46
20.5	0.333	2.14	1.94	146	6.72
33.0	0.208	3.45	3.14×10^5	116	6.82×10^3

TABLE VII

Run No. 203
$1\frac{1}{4}$" dia. half round wooden strips $\epsilon = 0.104$ ft.
Water depth: 1.892 ft. Water temp.: 66°F
Kinematic Viscosity: $\gamma = 1.09 \times 10^{-5}$ ft.²/sec.

cpm	Total Displacement d_1 ft	Angular Velocity ω rad/sec.	$\frac{\omega}{\gamma}$ $\frac{1}{ft^2}$	$\frac{\omega^{\frac{1}{2}} d_1}{\gamma^{\frac{1}{2}}}$	$\frac{\omega d_1 \epsilon}{\gamma}$
1.91	4.0	0.200	0.183×10^5	540	7.62×10^3
2.41	3.667	0.252	0.231	556	8.82
2.96	3.167	0.310	0.285	534	9.4
3.59	2.667	0.376	0.345	495	9.58
4.48	2.167	0.470	0.432	449	9.7
5.41	1.667	0.567	0.520	380	9.0
6.94	1.167	0.727	0.667	301	8.1
9.23	0.833	0.966	0.887	248	7.7
13.6	0.500	1.42	1.305	180	6.78
23.1	0.333	2.42	2.220	157	7.7
34.2	0.208	3.58	3.29×10^5	109	7.12×10^3

TABLE VIII

Run No. 301
¾ " dia. half round wooden strips $\epsilon = 0.0625$ ft.
Water depth: 0.528 ft. Water temp.: 64° F
Kinematic Viscosity: $\gamma = 1.12 \times 10^{-5}$ ft²/sec.

cpm	Total Displacement d_1 ft	Angular Velocity ω rad/sec	$\frac{\omega}{\gamma}$ $\frac{1}{ft^2}$	$\frac{\omega^{\frac{1}{2}} d_1}{\gamma^{\frac{1}{2}}}$	$\frac{\omega d_1 \epsilon}{\gamma}$
2.31	4.0	0.241	0.215×10^5	587	5.37×10^3
2.86	3.5	0.299	0.267	570	5.83
3.46	3.0	0.361	0.322	538	6.03
3.97	2.5	0.414	0.37	480	5.77
4.37	2.0	0.446	0.398	422	4.97
6.82	1.5	0.712	0.635	377	5.95
8.67	1.167	0.905	0.808	331	5.90
10.8	0.833	1.13	1.01	275	5.47
20.6	0.500	2.15	1.92	219	5.98
27.8	0.333	2.90	2.59	169	5.38
30.9	0.208	3.23	2.88×10^5	112	3.75×10^3

TABLE IX

Run No. 302
¾ " dia. half round wooden strips $\epsilon = 0.0625$ ft.
Water depth: 1.164 ft. Water temp.: 64°F
Kinematic Viscosity: $\gamma = 1.12 \times 10^{-5}$ ft²/sec.

cpm	Total Displacement $\frac{d_1}{ft}$	Angular Velocity ω rad/sec.	$\frac{\omega}{\gamma}$ $\frac{1}{ft^2}$	$\frac{\omega^{\frac{1}{2}} d_1}{\gamma^{\frac{1}{2}}}$	$\frac{\omega d_1 \epsilon}{\gamma}$
2.55	3.833	0.267	0.239×10^5	600	5.79×10^3
3.08	3.333	0.322	0.287	528	5.62
3.55	2.833	0.372	0.332	516	5.86
3.89	2.333	0.407	0.363	443	5.30
5.26	1.833	0.55	0.49	407	5.62
6.45	1.333	0.675	0.602	327	5.02
8.17	1.00	0.855	0.762	276	4.76
12.5	0.667	1.31	1.17	228	4.88
22.8	0.333	2.39	2.13	154	4.43
30.0	0.208	3.14	2.80×10^5	110	3.64×10^3

TABLE X

Run No. 303
¾" dia. half round wooden strips $\epsilon = 0.0625$ ft.
Water depth: 1.780 ft. Water temp.: 65°F
Kinematic Viscosity: $\gamma = 1.1 \times 10^{-5}$ ft²/sec.

cpm	Total Displacement d_1 ft	Angular Velocity ω rad/sec.	$\frac{\omega}{\gamma}$ $\frac{1}{ft^2}$	$\frac{\omega^{\frac{1}{2}} d_1}{\gamma^{\frac{1}{2}}}$	$\frac{\omega d_1 \epsilon}{\gamma}$
2.31	3.667	0.241	0.219×10^5	532	5.02×10^3
3.31	3.167	0.346	0.315	562	6.43
3.72	2.667	0.389	0.353	502	5.87
4.92	2.167	0.513	0.447	458	6.03
5.40	1.667	0.564	0.491	368	5.12
7.70	1.167	0.805	0.732	315	5.33
10.6	0.833	1.11	1.01	265	5.27
15.3	0.500	1.60	1.45	190	4.53
25.7	0.333	2.69	2.45	165	5.1
28.8	0.208	3.01	2.73×10^5	109	3.55×10^3

TABLE XI

Run No. 401
⅜" dia. half round wooden strips $\epsilon = 0.0312$ ft.
Water depth: 0.445 ft. Water temp.: 70°F
Kinematic Viscosity: $\gamma = 1.05\ 10^{-5}$ ft²/sec.

cpm	Total Displacement d_1 ft.	Angular Velocity ω rad/sec	$\frac{\omega}{\gamma}$ $\frac{1}{ft^2}$	$\frac{\omega^{\frac{1}{2}} d_1}{\gamma^{\frac{1}{2}}}$	$\frac{\omega d_1 \epsilon}{\gamma}$
2.27	4.0	0.237	0.226×10^5	600	2.86×10^3
2.53	3.5	0.265	0.251	556	2.75
3.16	3.0	0.331	0.315	533	2.96
3.52	2.5	0.368	0.35	467	2.74
4.8	2.0	0.502	0.477	436	2.98
6.32	1.5	0.662	0.63	376	2.96
9.23	1.0	0.965	0.92	303	2.87
14.1	0.667	1.475	1.40	249	2.92
22.5	0.333	2.35	2.24	158	2.33
30.3	0.208	3.17	3.01×10^5	114	1.96×10^3

TABLE XII

Run No. 402
3/8" dia. half round wooden strips $\epsilon = 0.0312$ ft.
Water depth: 1.124 ft. Water temp.: 70°F
Kinematic Viscosity: $\gamma = 1.05 \times 10^{-5}$ ft²/sec.

cpm	Total Displacement d_1 ft.	Angular Velocity ω rad/sec	$\frac{\omega}{\gamma}$ $\frac{1}{ft^2}$	$\frac{\omega^{\frac{1}{2}} d_1}{\gamma^{\frac{1}{2}}}$	$\frac{\omega d_1 \epsilon}{\gamma}$
2.55	3.833	0.267	0.255×10^5	611	3.05×10^3
2.81	3.333	0.294	0.28	557	2.92
3.43	2.833	0.359	0.342	523	3.03
3.76	2.333	0.393	0.374	451	2.73
5.31	1.833	0.556	0.528	422	3.03
7.64	1.333	0.800	0.762	367	3.17
12.1	0.833	1.265	1.205	289	3.13
15.6	0.500	1.63	1.56	198	2.46
35.3	0.208	3.18	3.03×10^5	114	1.98×10^3

TABLE XIII

Run No.403
3/8" dia. half round wooden strips $\epsilon = 0.0312$ ft.
Water depth: 1.798 Water temp.: 69°F
Kinematic Viscosity: $\gamma = 1.06 \times 10^{-5}$ ft²/sec.

cpm	Total Displacement d_1 ft.	Angular Velocity ω rad/sec.	$\frac{\omega}{\gamma}$ $\frac{1}{ft^2}$	$\frac{\omega^{\frac{1}{2}} d_1}{\gamma^{\frac{1}{2}}}$	$\frac{\omega d_1 \epsilon}{\gamma}$
2.31	4.0	0.242	0.227×10^5	600	2.84×10^3
2.97	3.167	0.311	0.293	543	2.90
4.69	2.167	0.49	0.462	466	3.12
6.13	1.667	0.642	0.605	410	3.14
8.76	1.167	0.916	0.863	342	3.16
15.0	0.667	1.57	1.48	256	3.08
23.1	0.333	2.42	2.28	159	2.37
31.9	0.208	3.34	3.15×10^5	117	2.05×10^3

TABLE XIV

Run NO. 501
3/64" dia. round steel rods $\epsilon = 0.0039$ ft.
Water depth: 1.258 ft. Water temp.: 69°F
Kinematic Viscosity: $\gamma = 1.06 \times 10^{-5}$ ft²/sec.

cpm	Total Displacement d_1 ft.	Angular Velocity ω rad./sec.	$\frac{\omega}{\gamma}$ $\frac{1}{ft^2}$	$\frac{\omega^{1/2} d_1}{\gamma^{1/2}}$	$\frac{\omega d_1 \epsilon}{\gamma}$
4.43	3.833	0.463	0.447×10^5	806	0.667×10^3
5.36	3.333	0.563	0.532	768	0.691
6.97	2.833	0.728	0.686	743	0.781
9.23	2.333	0.965	0.91	702	0.827
11.5	1.833	1.20	1.13	617	0.808
20.4	1.333	2.13	2.01	597	1.045
31.4	1.00	3.28	3.09	555	1.205
53.3	0.667	5.57	5.25	483	1.365
99.3	0.333	10.4	9.82	330	1.275
30.0	1.167	3.13	2.95	633	1.345
40.6	0.833	4.24	4.0	526	1.30
82.7	0.500	8.65	8.16×10^5	451	$1.59 \quad 10^3$

TABLE XV

Run NO. 502
5/64" dia. round steel rods $\epsilon = 0.0039$ ft.
Water depth: 0.552 ft. Water temp.: 69°F
Kinematic Viscosity: $\gamma = 1.06 \times 10^{-5}$ ft²/sec.

cpm	Total Displacement d_1 ft.	Angular Velocity ω rad./sec.	$\frac{\omega}{\gamma}$ $\frac{1}{ft^2}$	$\frac{\omega^{1/2} d_1}{\gamma^{1/2}}$	$\frac{\omega d_1 \epsilon}{\gamma}$
8.8	2.5	0.918	$0.865 \quad 10^5$	733	$0.822 \quad 10^3$
13.5	2.0	1.41	1.33	728	1.035
18.5	1.5	1.93	1.82	640	1.065
28.5	1.0	2.98	2.81	528	1.095
44.2	0.667	4.61	4.33	438	1.125
93.3	0.333	9.73	9.16	319	1.185
4.36	4.0	0.455	0.429	828	0.67
6.3	3.5	0.657	0.618	667	0.845
7.12	3.0	0.743	0.702×10^5	790	0.820×10^3

TABLE XVI

Run NO. 503
3/64" dia. round steel rods $\epsilon = 0.0039$ ft.
Water depth: 1.821 ft. Water temp.: 71°F
Kinematic Viscosity: $\gamma = 1.03 \times 10^{-5}$ ft²/sec.

cpm	Total Displacement d_1 ft.	Angular Velocity ω rad./sec.	$\frac{\omega}{\gamma}$ $\frac{1}{ft^2}$	$\frac{\omega^{1/2} d_1}{\gamma^{1/2}}$	$\frac{\omega d_1 \epsilon}{\gamma}$
5.48	3.667	0.575	0.557×10^5	862	0.822×10^3
6.25	3.167	0.655	0.636	797	0.786
7.76	2.667	0.813	0.79	760	0.822
9.47	2.167	0.992	0.962	682	0.812
12.2	1.667	1.28	1.24	595	0.807
27.7	1.167	2.90	2.81	618	1.28
38.2	3.833	4.00	3.88	527	1.26
56.2	0.50	5.88	5.72×10^5	378	1.11×10^3

III. Rough Bottom - Sand and Gravel

TABLE XVII

Run NO. 601
Average sand size: 0.00308 ft.
D_{50}=0.00308 ft. D_{35}=0.00283 ft. D_{65}=0.00315 ft.
Water depth: 0.283 ft. Water temp.: 61°F
Kinematic Viscosity: $\gamma = 1.19 \times 10^{-5}$ ft²/sec.

cpm	Total Displacement d_1 ft.	Angular Velocity ω rad./sec.	$\frac{\omega}{\gamma}$ $\frac{1}{ft^2}$	$\frac{\omega^{1/2} d_1}{\gamma^{1/2}}$	$\frac{\omega d_1 \epsilon}{\gamma}$
3.26	4.0	0.341	0.281×10^5	670	0.346×10^3
3.95	3.5	0.413	0.348	652	0.374
4.76	3.0	0.498	0.418	613	0.387
4.96	2.5	0.521	0.438	523	0.339
6.74	2.0	0.704	0.592	465	0.365
8.76	1.5	0.916	0.770	416	0.355
15.1	1.0	1.58	1.325	363	0.408
22.2	0.667	2.32	1.95	294	0.402
37.5	0.333	3.92	3.29	191	0.337
56.1	0.208	5.66	4.92×10^5	146	0.315×10^3

TABLE XVIII

Run NO. 602
Average sand size: 0.00308 ft.
D_{50}=0.00308 ft. D_{35}=0.00283 ft. D_{65}=0.00315 ft.
Water depth: 0.834 ft. Water temp.: 61° F
Kinematic Viscosity: $\gamma = 1.19 \times 10^{-5}$ ft²/sec.

cpm	Total Displacement d_1 ft.	Angular Velocity ω rad./sec.	$\frac{\omega}{\gamma}$ $\frac{1}{ft^2}$	$\frac{\omega^{1/2} d_1}{\gamma^{1/2}}$	$\frac{\omega d_1 \epsilon}{\gamma}$
3.86	3.833	0.403	0.339×10^5	706	0.40×10^3
4.72	3.333	0.493	0.414	677	0.426
4.90	2.833	0.512	0.430	586	0.375
5.71	2.333	0.596	0.501	521	0.360
7.65	1.833	0.799	0.672	474	0.379
11.6	1.333	1.21	1.015	424	0.417
18.6	0.833	1.9	1.63	336	0.418
26.6	0.500	2.78	2.33	241	0.359
43.9	0.333	4.58	3.85	207	0.395
55.0	0.208	5.74	4.82×10^5	144	0.309×10^3

TABLE XIX

Run NO. 603
Average sand size: 0.00308 ft.
D_{50}=0.00308 ft. D_{35}=0.00283 ft. D_{65}=0.00315 ft.
Water depth: 1.576 ft. Water temp.: 62° F
Kinematic Viscosity: $\gamma = 1.17 \times 10^{-5}$ ft²/sec.

cpm	Total Displacement d_1 ft.	Angular Velocity ω rad./sec.	$\frac{\omega}{\gamma}$ $\frac{1}{ft^2}$	$\frac{\omega^{1/2} d_1}{\gamma^{1/2}}$	$\frac{\omega d_1 \epsilon}{\gamma}$
3.64	3.667	0.384	0.328×10^5	663	0.359×10^3
4.15	3.167	0.433	0.371	609	0.362
5.09	2.667	0.532	0.453	568	0.372
6.25	2.167	0.653	0.558	512	0.375
7.06	1.667	0.736	0.632	418	0.325
10.4	1.167	1.09	0.832	335	0.299
11.9	1.00	1.245	1.065	326	0.326
15.0	0.833	1.57	1.340	305	0.343
21.3	0.667	2.23	1.905	291	0.392
25.4	0.500	2.26	2.27	237	0.350
36.3	0.333	3.80	3.25	190	0.334
57.7	0.208	6.03	5.17×10^5	150	0.331×10^3

TABLE XX

Run NO. 701
Gravel size: 0.0453 ft.
Water depth: 0.673 ft. Water temp.: 63°F
Kinematic Viscosity: $\gamma = 1.15 \times 10^{-5}$ ft.^{2}/sec.

cpm	Total Displacement d_1 ft.	Angular Velocity ω rad/sec	$\frac{\omega}{\gamma}$ $\frac{1}{ft^2}$	$\frac{\omega^{\frac{1}{2}} d_1}{\gamma^{\frac{1}{2}}}$	$\frac{\omega d_1 \epsilon}{\gamma}$
1.85	3.667	0.194	0.169×10^5	477	2.81×10^3
2.18	3.167	0.228	0.198	445	2.84
2.93	2.667	0.307	0.267	435	3.23
3.68	2.167	0.387	0.337	397	3.31
4.22	1.667	0.442	0.384	326	2.90
5.10	1.333	0.534	0.463	287	2.81
6.25	1.00	0.654	0.568	238	2.58
10.4	0.667	1.090	0.948	205	2.87
15.7	0.50	1.645	1.430	189	3.24
23.1	0.333	2.42	2.11	153	3.18
32.2	0.208	3.48	3.03×10^5	115	2.86×10^3

TABLE XXI

Run NO. 702
Gravel size: 0.0453 ft. Water depth: 1.327 ft.
Water temp.: 63° F Kinematic Viscosity: $\gamma = 1.15 \times 10^{-5}$ ft²/sec

cpm	Total Displacement d_1 ft	Angular Velocity ω rad/sec	$\frac{\omega}{\gamma}$ $\frac{1}{ft^2}$	$\frac{\omega^{\frac{1}{2}} d_1}{\gamma^{\frac{1}{2}}}$	$\frac{\omega d_1 \epsilon}{\gamma}$
1.62	4.0	0.169	0.147×10^5	483	2.67×10^3
2.36	3.0	0.247	0.215	438	2.93
2.55	2.5	0.267	0.232	380	2.63
3.68	2.0	0.385	0.335	366	3.04
4.31	1.667	0.451	0.391	329	2.95
5.41	1.333	0.566	0.492	295	2.96
6.65	1.000	0.695	0.604	245	2.74
8.86	0.667	0.926	0.805	189	2.43
1.67	3.833	0.175	0.152	470	2.64
2.11	3.333	0.221	0.192	462	2.90
2.40	2.833	0.251	0.219	418	2.82
3.82	2.333	0.399	0.347	433	3.67
4.09	1.833	0.427	0.371	353	3.08
6.21	1.333	0.650	0.565	317	3.42
6.52	1.167	0.682	0.593	284	3.14
7.76	1.000	0.812	0.706	265	3.20
8.65	0.833	0.893	0.777	229	2.94
10.3	0.667	1.075	0.935	204	2.84
12.4	0.50	1.295	1.125	167	2.56
16.3	0.333	1.705	1.485	128	2.25
27.0	0.208	2.82	2.45×10^5	103	2.31×10^3

TABLE XXII

Run NO. 703
Gravel size: 0.0453 ft. Water depth: 1.967 ft.
Water temp.: 62 F Kinematic Viscosity: $\gamma = 1.17 \times 10^{-5}$ ft²/sec

cpm	Total Displacement d_1 ft	Angular Velocity ω rad/sec	$\frac{\omega}{\gamma}$ $\frac{1}{ft^2}$	$\frac{\omega^{\frac{1}{2}} d_1}{\gamma^{\frac{1}{2}}}$	$\frac{\omega d_1 \epsilon}{\gamma}$
1.79	3.833	0.187	0.160×10^5	485	2.78×10^3
2.30	3.333	0.241	0.206	477	3.12
2.48	2.833	0.260	0.222	421	2.85
3.02	2.333	0.316	0.270	383	2.86
4.51	1.833	0.472	0.403	368	3.37
6.43	1.333	0.673	0.573	319	3.40
9.09	1.000	0.950	0.812	285	3.67
9.23	0.833	0.966	0.826	239	3.12
10.6	0.667	1.110	0.948	205	2.87
14.4	0.500	1.515	1.295	180	2.93
26.1	0.333	2.73	2.33	161	3.52
34.1	0.208	3.57	3.05×10^5	115	2.89×10^3

TABLE XXIII

Run NO. 801
Average sand size: 0.0009 ft.
D_{50}=0.0009 ft. D_{35}=0.00084 ft. D_{65}=0.00098 ft.
Water depth: 1.896 ft. Water temp.: 75.5°F
Kinematic Viscosity: $\gamma = 0.96 \times 10^{-5}$ ft²/sec.

cpm	Total Displacement d_1 ft	Angular Velocity ω rad/sec	$\frac{\omega}{\gamma}$ $\frac{1}{ft^2}$	$\frac{\omega^{\frac{1}{2}} d_1}{\gamma^{\frac{1}{2}}}$	$\frac{\omega\, d_1 \epsilon}{\gamma}$
4.05	4.0	0.422	0.446×10^5	843	1.605×10^2
5.2	3.5	0.542	0.565	832	1.78
5.88	3.0	0.613	0.628	753	1.69
7.23	2.5	0.755	0.785	700	1.77
10.3	2.0	1.075	1.12	668	2.01
13.3	1.5	1.395	1.445	550	1.95
19.2	1.0	2.00	2.08	467	1.87
32.0	0.667	3.33	3.47×10^5	393	2.08×10^2

TABLE XXIV

Run NO. 802
Average sand size: 0.0009 ft.
D 0.0009 ft. D 0.00084 ft. D 0.00098 ft.
Water depth: 1.896 ft. Water temp.: 75.5°F
Kinematic Viscosity: $\gamma = 0.96 \times 10^{-5}$ ft²/sec.

cpm	Total Displacement d_1 ft	Angular Velocity ω rad/sec.	$\frac{\omega}{\gamma}$ $\frac{1}{ft^2}$	$\frac{\omega^{\frac{1}{2}} d_1}{\gamma^{\frac{1}{2}}}$	$\frac{\omega\, d_1 \epsilon}{\gamma}$
4.41	3.833	0.460	0.478×10^5	837	1.655×10^2
5.40	3.333	0.563	0.587	805	1.76
7.23	2.833	0.755	0.786	794	1.65
9.09	2.333	0.948	0.987	730	2.07
10.6	1.833	1.105	1.15	621	1.90
14.4	1.333	1.50	1.56	527	1.87
24.0	0.833	2.51	2.61	426	1.88
43.6	0.500	4.56	4.73	344	2.13
60.7	0.333	6.33	6.60	270	1.98
18.4	1.167	1.92	2.01	525	2.11
29.4	0.667	3.07	3.27	373	1.92
44.5	0.500	4.63	4.86	347	2.19
65.3	0.333	6.82	7.10×10^5	280	2.13×10^2

TABLE XXV

Run NO. 901
Polystyrene pellet:
$\epsilon = 0.0104$ ft.
Water depth: 1.905 ft. Water temp.: 76°F
Kinematic Viscosity: $\gamma = 0.95 \times 10^{-5}$ ft²/sec.

cpm	Total Displacement d_1 ft	Angular Velocity ω rad./sec.	$\frac{\omega}{\gamma}$ $\frac{1}{ft^2}$	$\frac{\omega^{1/2} d_1}{\gamma^{1/2}}$	$\frac{\omega d_1 \epsilon}{\gamma}$
2.37	4.0	0.248	0.253×10^5	637	1.055×10^3
2.85	3.5	0.299	0.315	620	1.14
3.59	3.0	0.376	0.396	597	1.24
4.07	2.5	0.427	0.448	528	1.11
4.68	2.0	0.491	0.517	455	1.075
6.38	1.5	0.668	0.703	400	1.10
8.90	1.0	0.932	0.982	313	1.02
12.40	0.667	1.30	1.365	289	0.948
25.30	0.333	2.65	2.80×10^5	176	0.97×10^3

TABLE XXVI

Run NO. 902
Polystyrene pellet:
$\epsilon = 0.0104$ ft.
Water depth: 1.905 ft. Water temp.: 76°F
Kinematic Viscosity: $\gamma = 0.95 \times 10^{-5}$ ft²/sec.

cpm	Total Displacement d_1 ft.	Angular Velocity ω rad./sec.	$\frac{\omega}{\gamma}$ $\frac{1}{ft^2}$	$\frac{\omega^{1/2} d_1}{\gamma^{1/2}}$	$\frac{\omega d_1 \epsilon}{\gamma}$
2.57	3.667	0.269	0.295×10^5	630	1.125×10^3
3.11	3.167	0.326	0.345	587	1.135
3.73	2.667	0.389	0.413	542	1.145
4.22	2.167	0.442	0.467	468	1.05
5.48	1.667	0.575	0.603	408	1.05
7.68	1.167	0.805	0.847	339	1.03
12.2	0.833	1.28	1.34	305	1.165
17.15	0.500	1.80	1.94	220	1.01
32.2	0.208	3.38	3.54×10^5	124	0.766×10^3